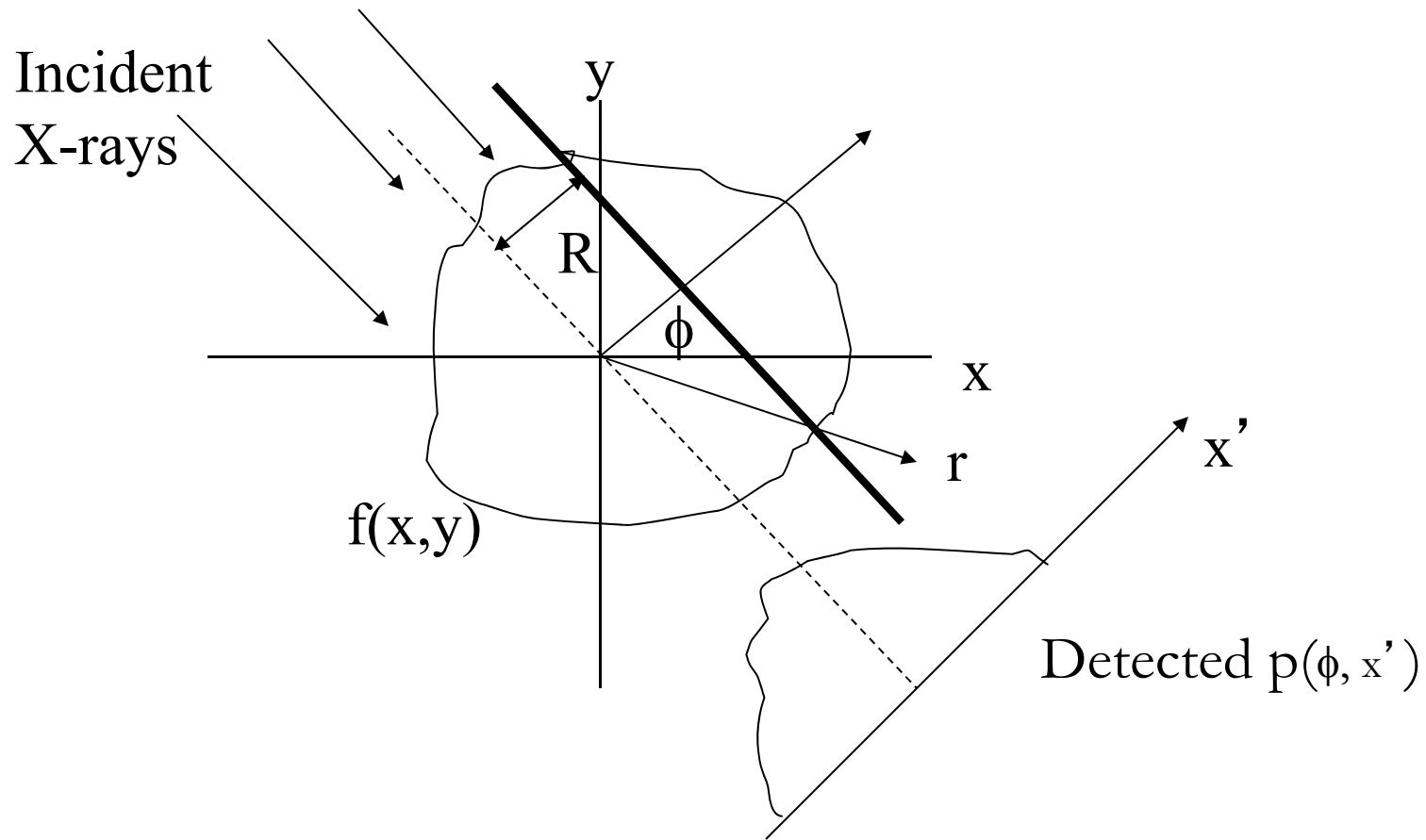


Central Slice Theorem



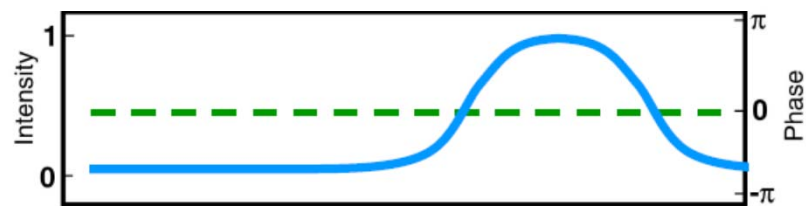
The thick line is described by

$$x \cos \phi + y \sin \phi = R$$

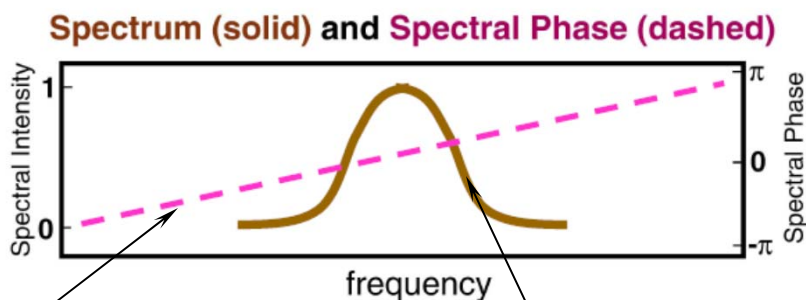
Properties of Fourier Transform

$$\mathcal{F}[f(x-a)] = \mathcal{F}[f(x)]e^{-j2\pi\cdot\omega\cdot a}$$

Spatial Domain



Spatial Frequency Domain



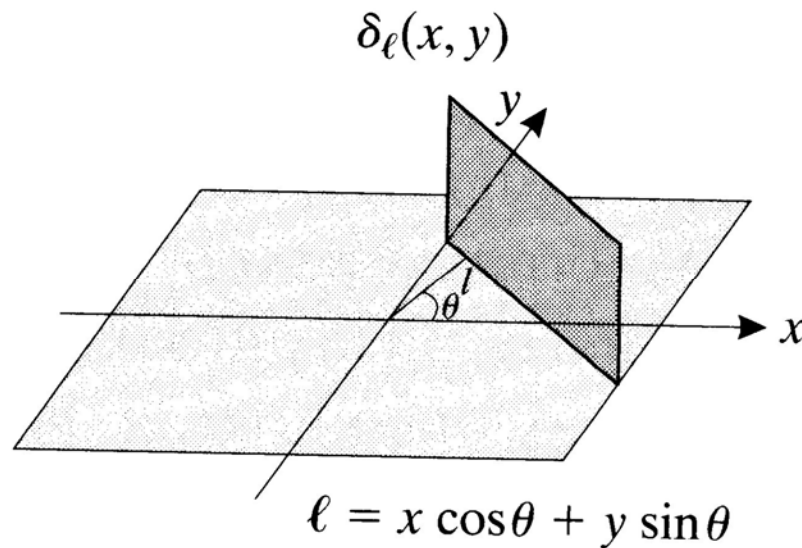
Linear shifting in spatial domain
simply adds some linear phase to
the pulse

Magnitude is unchanged

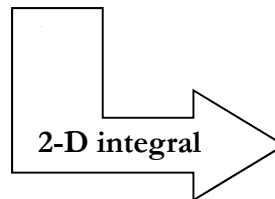
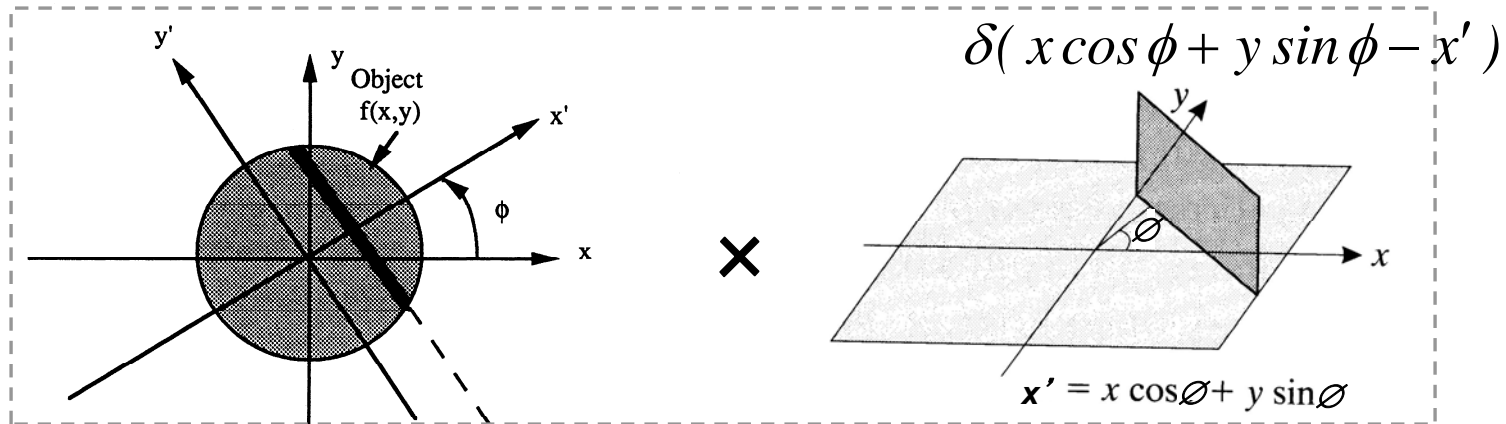
Line Impulse Signal (1)

$$\delta_L(x, y) = \delta(x \cos \theta + y \sin \theta - l)$$

where $\delta(x) = \begin{cases} > 0, & x \cos \theta + y \sin \theta = l \\ 0, & \text{otherwise} \end{cases}$



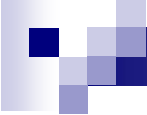
Line Impulse Signal (2)



The value of the projection function $p_\phi(x')$ at this point is the integral of the function of $f(x,y)$ along the straight line:
 $x' = x \cos \phi + y \sin \phi$

The integral of a line impulse function and a given 2-D signal gives the ***projection*** data from a given view ...

$$p(\phi, x') = \int_{-\infty}^{\infty} \int_{-\infty}^{\infty} f(x, y) \delta(x \cos \phi + y \sin \phi - x') dx dy$$



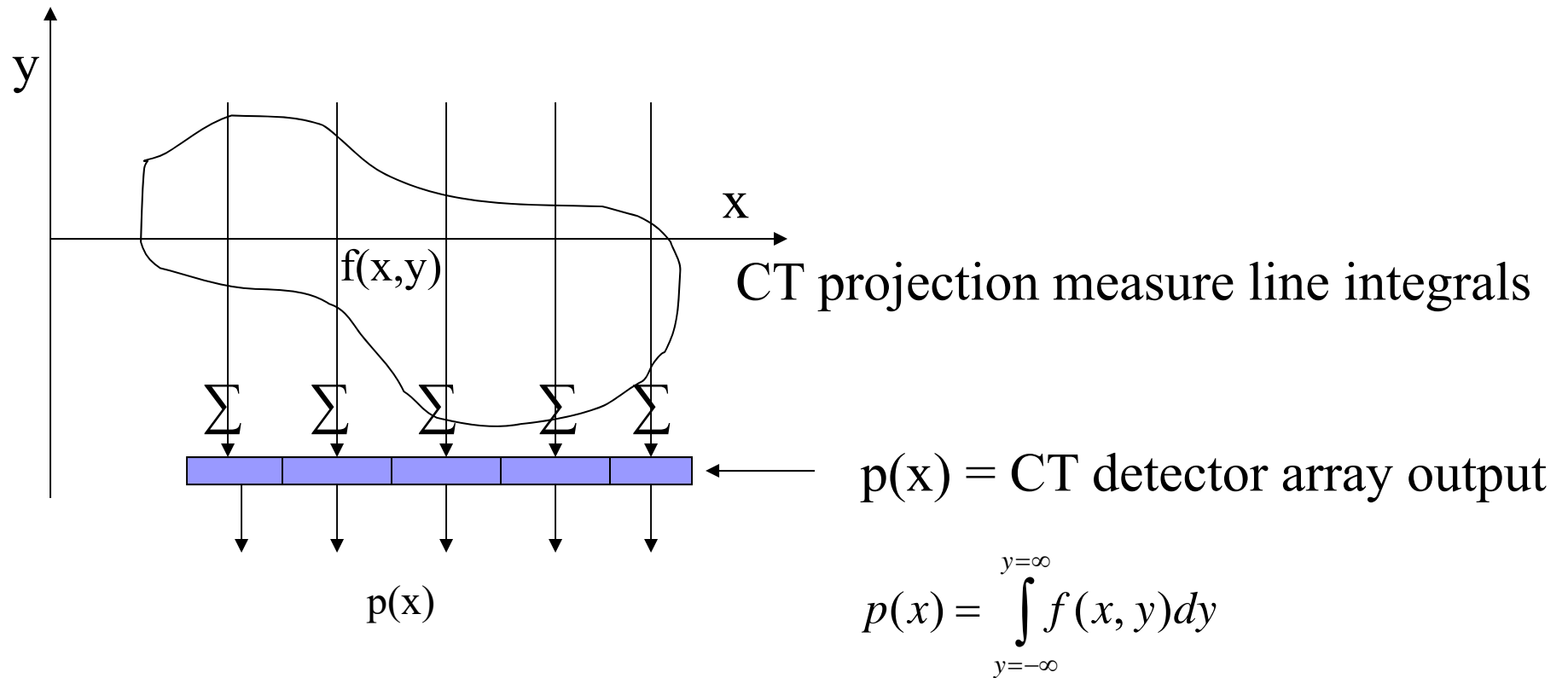
Central Section Or Projection Slice Theorem

$$F\{p(\phi, x')\} = F(r, \phi)$$

So in words, the Fourier transform of a projection at angle ϕ gives us a line in the polar Fourier space at the same angle ϕ .

Central slice theorem is the key to understand reconstructions from projection data

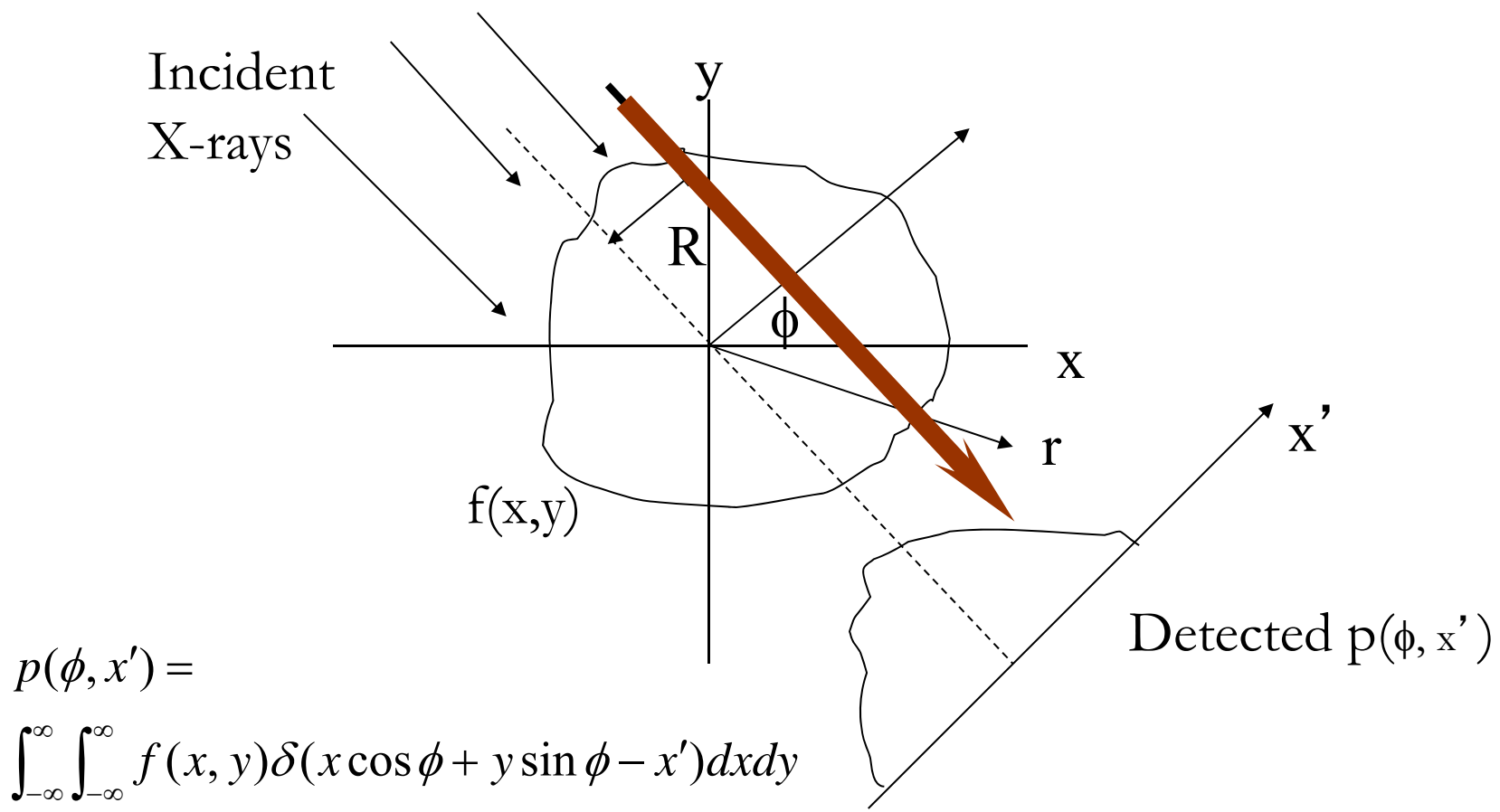
X-ray Projection Revisited



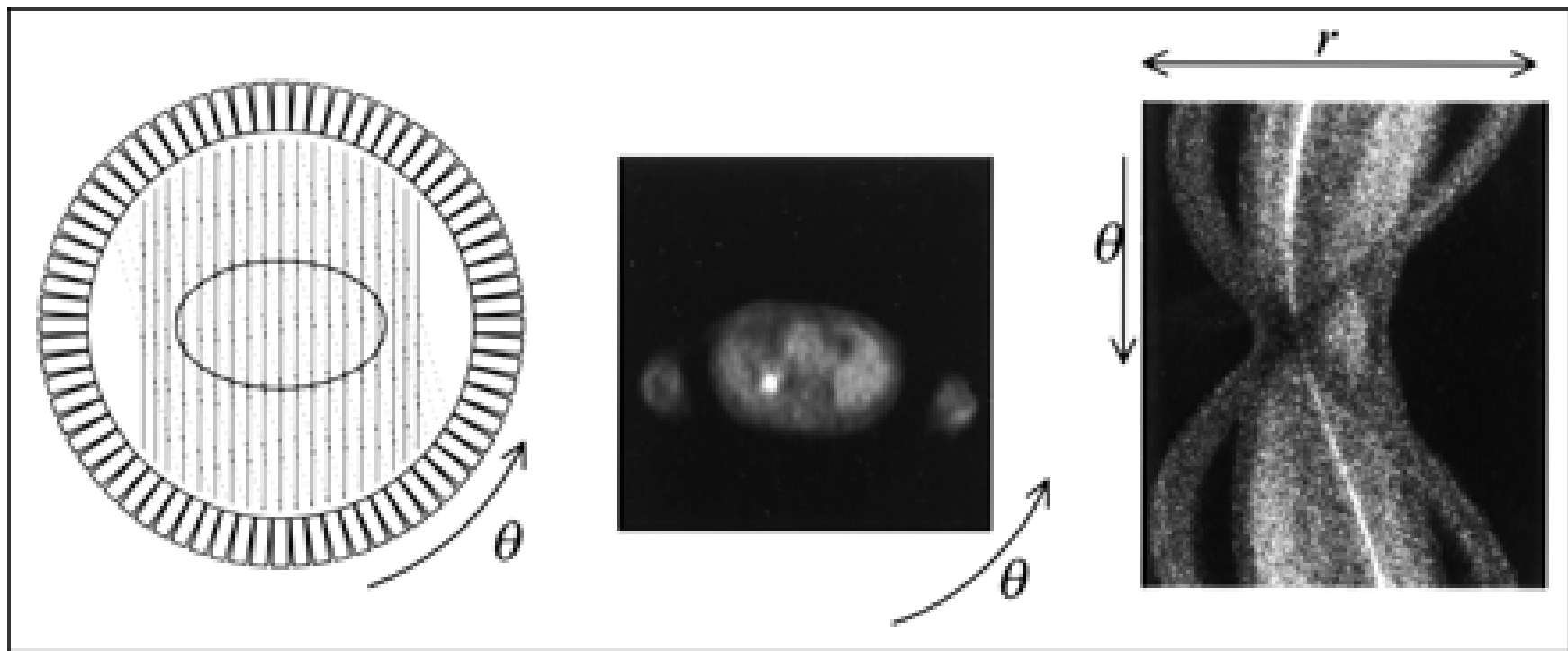
Review of 2-D Analytical Reconstruction Methods

Projection Data

Projection data $p(\phi, x')$

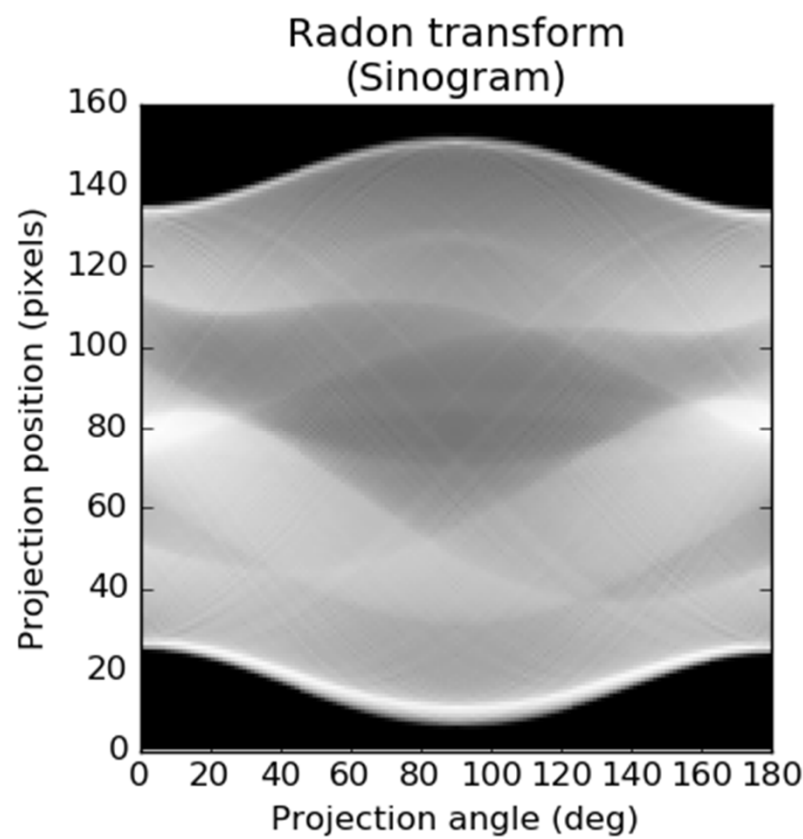
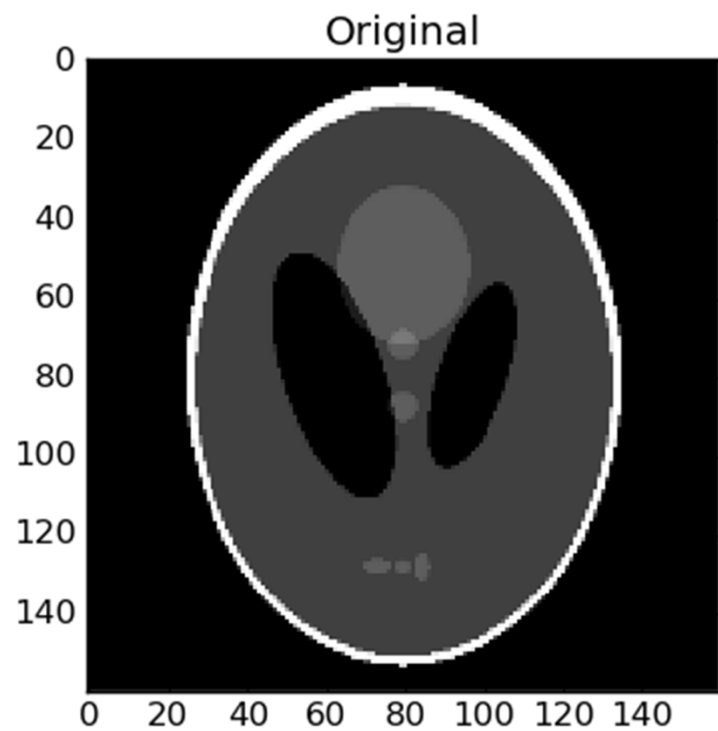


Radon Transform and Sinogram



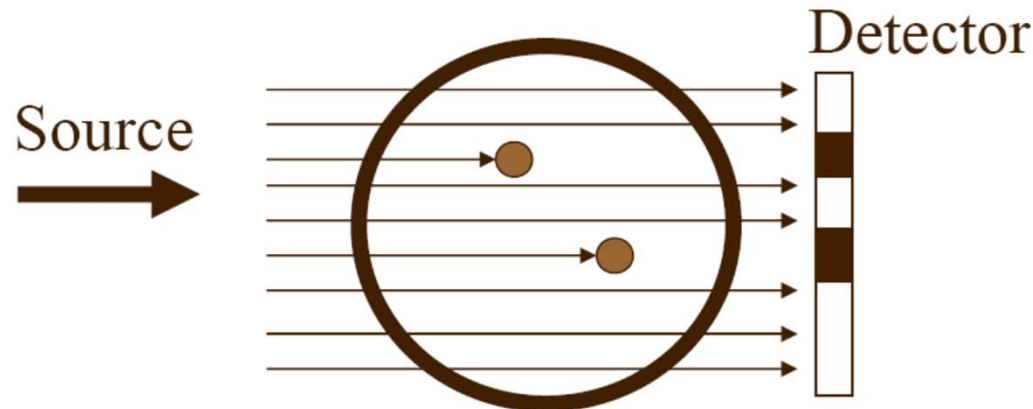
<http://tech.snmjournals.org/cgi/content-nw/full/29/1/4/F3>

Radon Transform and Sinogram



<http://tech.snmjournals.org/cgi/content-nw/full/29/1/4/F3>

Simple Backprojection

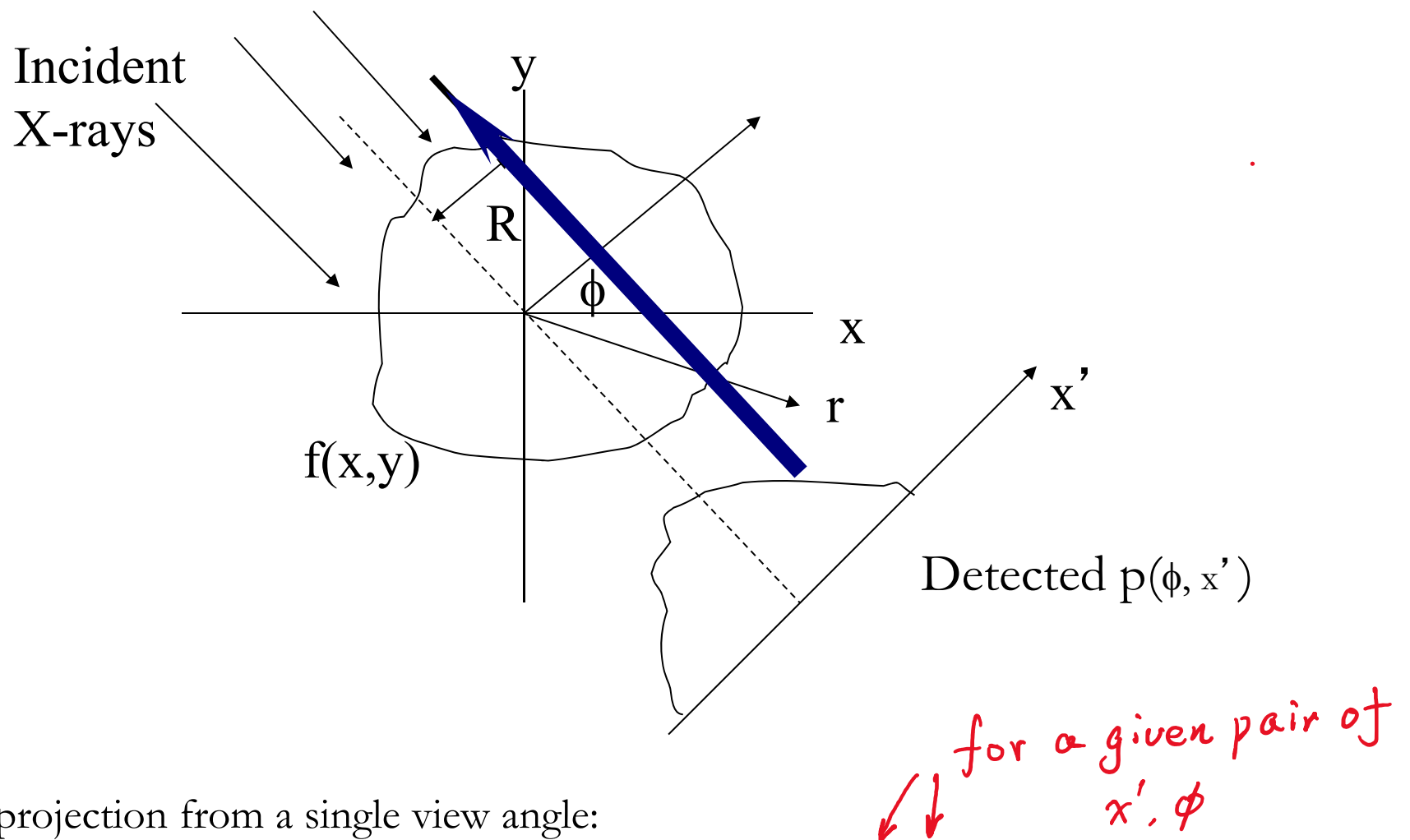


inverse = 1 back projection



Review of 2-D Analytical Reconstruction Methods

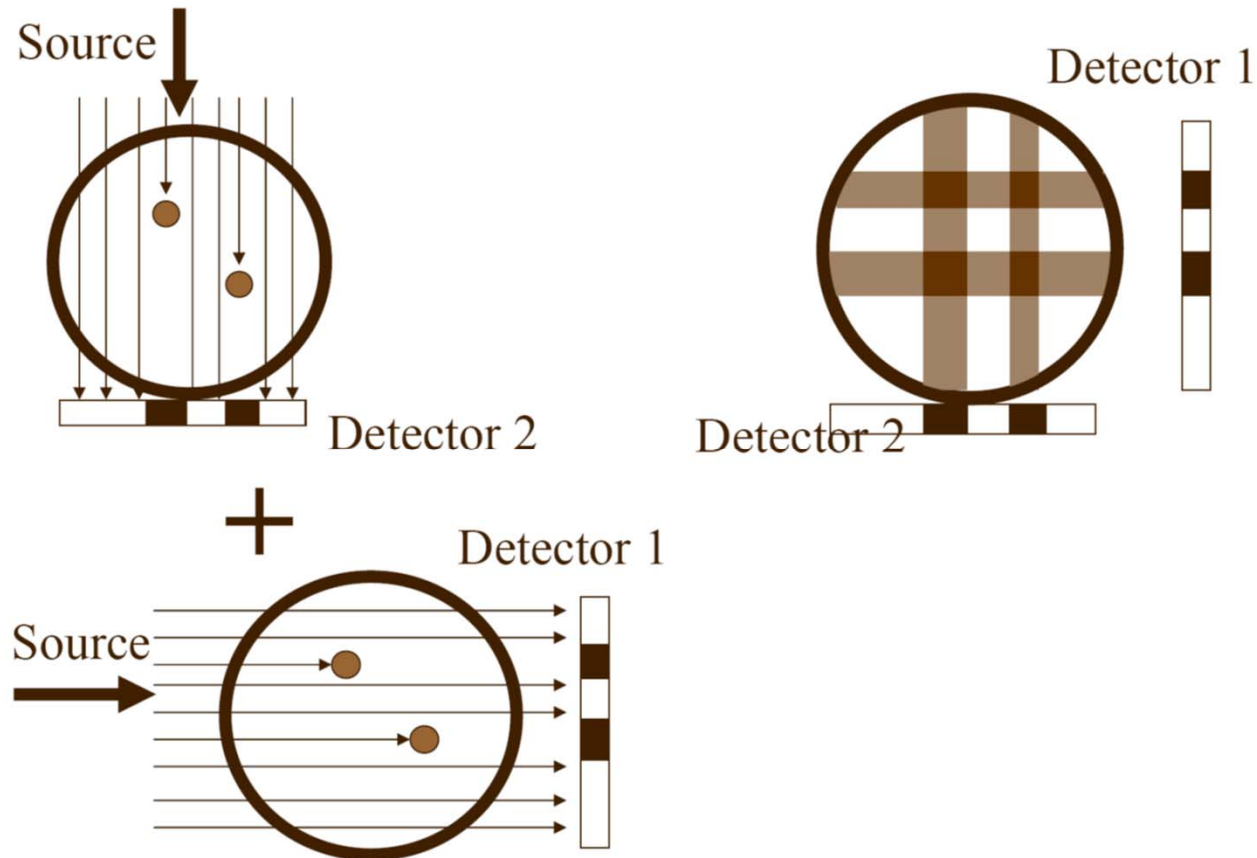
Back Projection Operation



Back projection from a single view angle:

$$b_\phi(x,y) = \int_{x'} p_\phi(x') \delta(x \cos \phi + y \sin \phi - x') dx'$$

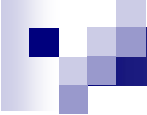
Simple Backprojection



Adding up all the back projections from all the angles gives,

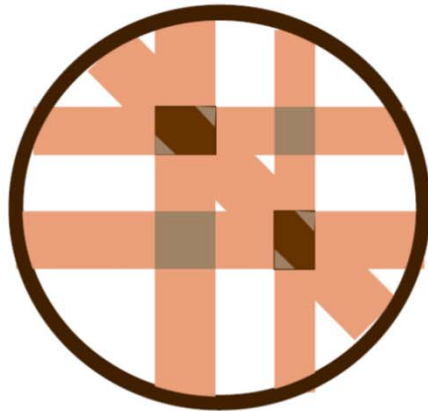
$$f_{\text{back-projected}}(x,y) = \int_{\phi} b_{\phi}(x,y) d\phi$$

$$f_b(x,y) = \int_{\phi=0}^{\pi} d\phi \int_{x'= -\infty}^{\infty} p_{\phi}(x') \delta(x \cos \phi + y \sin \phi - x') dx'$$

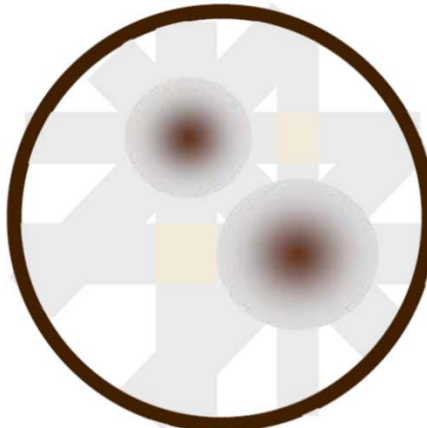


Simple Backprojection

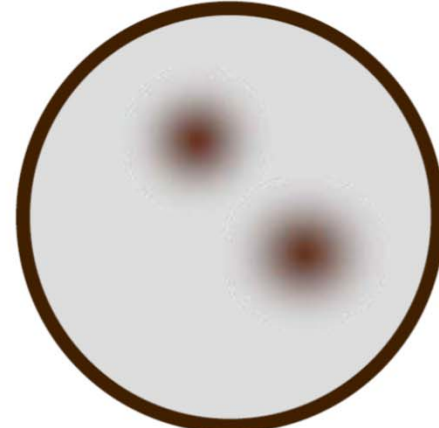
3 projections



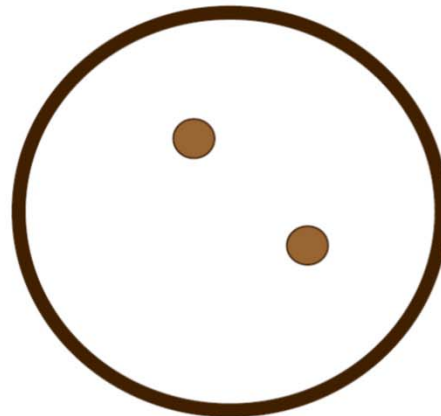
4 projections



many projections



Original
object



12

Simple Backprojection

Crude Idea 1: Take each projection and smear it back along the lines of integration it was calculated over.

Result from a back projection from a single view angle:

$$b_\phi(x, y) = \int_{x'} p_\phi(x') \delta(x \cos \phi + y \sin \phi - x') dx'$$

Adding up all the back projections from all the angles gives,

$$f_{\text{back-projected}}(x, y) = \int_{\phi} b_\phi(x, y) d\phi$$

$$f_b(x, y) = \int_0^\pi d\phi \int_{-\infty}^{\infty} p_\phi(x') \delta(x \cos \phi + y \sin \phi - x') dx'$$

Simple Back-projection and the $1/r$ Blurring

MP
BE
Medical Physics and Biomedical Engineering

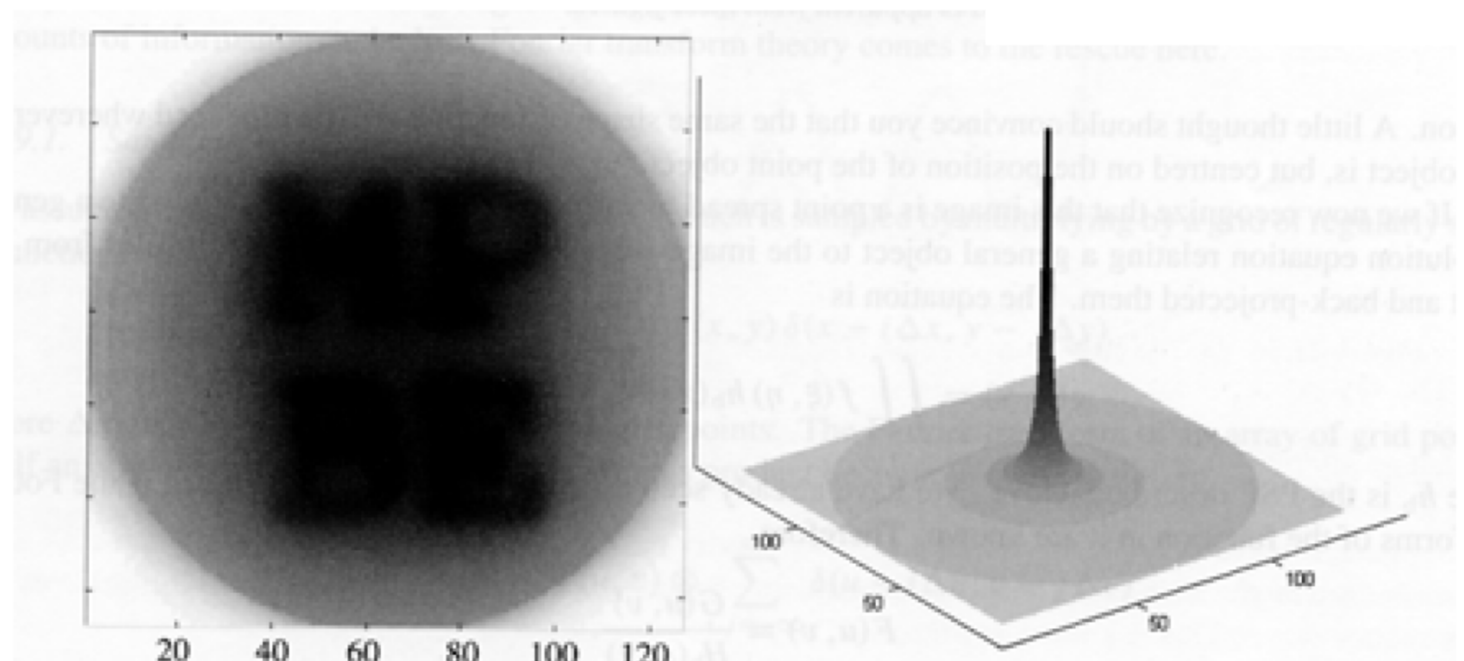


Figure 11.14. (a) Image produced by back-projecting the sinogram given in figure 11.12(b); (b) the response to a point object in the middle of the field of view.

From Medical Physics and Biomedical Engineering, Brown, IoP Publishing

Impulse Response Function of Simple Backprojection Operator

$$h_b(r) = 1/r$$

$$f_b(x,y) = f(x,y) * 1/r$$

$$F_b(\rho, \phi) = F(\rho, \phi) / \rho \quad \text{since } F\{1/r\} = 1/\rho$$

Back projected image is blurred by convolution with $1/r$

Simple Back-projection and the $1/r$ Blurring

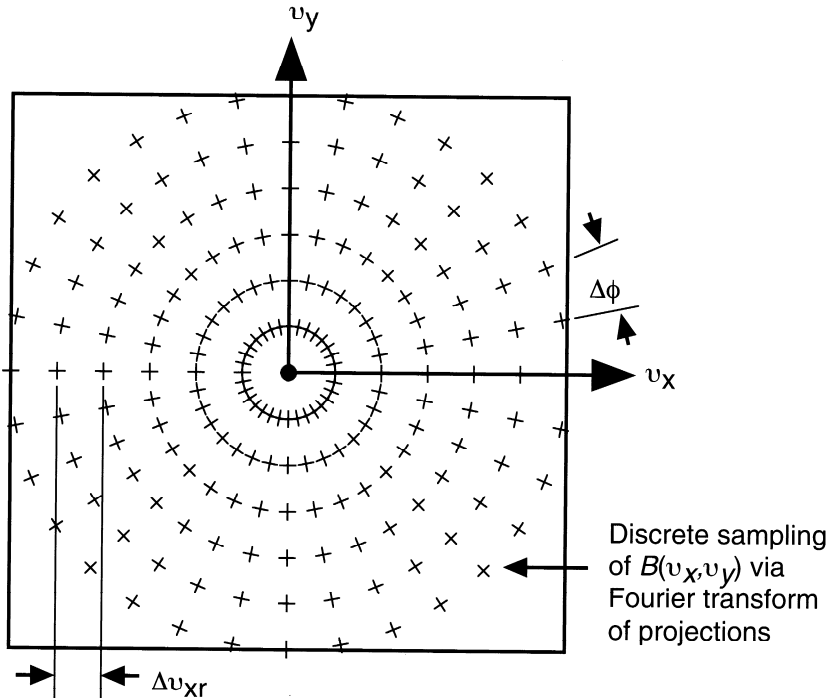


FIGURE 18 The discrete sampling pattern of $F(v_x, v_y)$ contained in $B(v_x, v_y)$, resulting from the use of discretely sampled projections.

**The nature of the $1/r$ blurring:
Radon transform produced equally spaced radial
sampling in Fourier domain.**

Simple Backprojection

Crude Idea 1: Take each projection and smear it back along the lines of integration it was calculated over.

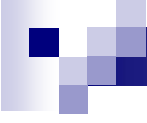
Result from a back projection from a single view angle:

$$b_\phi(x, y) = \int_{x'} p_\phi(x') \delta(x \cos \phi + y \sin \phi - x') dx'$$

Adding up all the back projections from all the angles gives,

$$f_{\text{back-projected}}(x, y) = \int b_\phi(x, y) d\phi$$

$$f_b(x, y) = \int_0^\pi d\phi \int_{-\infty}^{\infty} p_\phi(x') \delta(x \cos \phi + y \sin \phi - x') dx'$$



The Nature of the $1/r$ Blurring

The nature of the $1/r$ blurring:

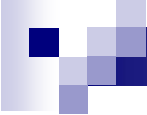
Radon transform produced equally spaced radial sampling in Fourier domain.

The low frequency components are over sampled, which causes

$$h_b(r) = 1/r \text{ and } f_b(x,y) = f(x,y) * 1/r \quad \text{in spatial domain}$$

and

$$F_b(\rho, \phi) = F(\rho, \phi) / \rho \quad \text{in spatial frequency domain}$$



Inverse Radon Transform

Suppose the sample projection data preserves all information contained in the original function $f(x,y)$, can we recover the exact function $f(x,y)$ with an ***Inverse Radon Transform***?

$$\mathcal{R}^{-1}\{\mathcal{R}[f(x, y)]\} = \hat{f}(x, y)$$

Inverse Radon Transform

The estimate of the original image $f(x,y)$ can be obtained as

$$\hat{f}(r, \theta) = \int_0^\pi \int_{-\infty}^\infty |\omega| P_\phi(\omega) \exp[i\omega(x \cos \phi + y \sin \phi)] d\omega d\phi$$

$$\quad\quad\quad = \int_0^\pi p_\phi^*(x') d\phi$$

$$\hat{f}(x, y) = \int_0^\pi d\phi \int_{-\infty}^\infty \underbrace{P_\phi^*(x')} \cdot \delta(x \cos \phi + y \sin \phi - x') dx'$$

where

$$\begin{aligned} p_\phi^*(x') &= \int_{-\infty}^\infty |\omega| P_\phi(\omega) \exp(i\omega x') d\omega \\ &= \mathcal{F}_1^{-1}[|\omega| P_\phi(\omega)] \\ &= \mathcal{F}_1^{-1}[|\omega|] * p_\phi(x') \quad \text{The Central Slice Theorem} \end{aligned}$$

and

$$\begin{aligned} P_\phi(\omega) &= F(\omega \cos \phi, \omega \sin \phi) \\ &= F(\omega_{x'}, \omega_{y'})|_\phi \quad \text{or} \quad F(\omega_x, \omega_y)|_\phi \\ &= F(\omega, \phi) \end{aligned}$$

Simple and Filtered Back-projection

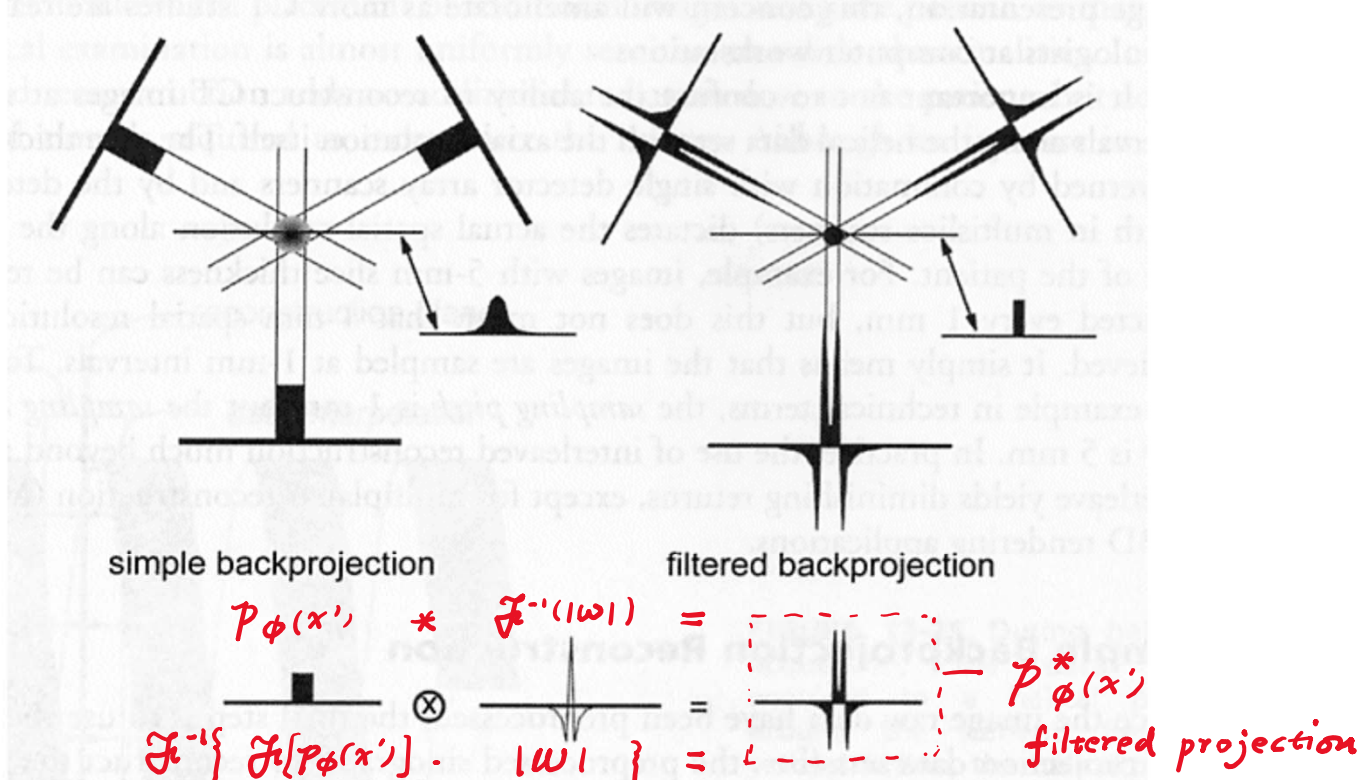


FIGURE 13-28. Simple backprojection is shown on the left; only three views are illustrated, but many views are actually used in computed tomography. A profile through the circular object, derived from simple backprojection, shows a characteristic $1/r$ blurring. With filtered backprojection, the raw projection data are convolved with a convolution kernel and the resulting projection data are used in the backprojection process. When this approach is used, the profile through the circular object demonstrates the crisp edges of the cylinder, which accurately reflects the object being scanned.

Chapters 12 & 13, The Essential Physics of Medical Imaging, Bushberg

Filtered Back-projection

Mathematically, we can define a *filtered back-projection* FBP operation to remove the $1/r$ blurring.

$$\hat{f}(x, y) = \frac{1}{\pi} \int_0^\pi d\phi \int_{-\infty}^{\infty} dx' p_\phi(x') h(x \cos \phi + y \sin \phi - x')$$

where

$$\begin{aligned} h(x') &= \mathcal{F}_1^{-1}[|\omega|] \\ &= \mathcal{F}_1^{-1}[H(\omega)] \end{aligned}$$

Can this be realized ??

Due to the diverging nature of the $|w|$ function, the corresponding filter kernel does not exist in spatial domain!

Inverse Radon Transform

The estimate of the original image $f(x,y)$ can be obtained as

$$\begin{aligned}\hat{f}(x, y) &= \hat{f}(r, \theta) = \boxed{\beta \mathcal{H}\{p_\phi(x')\}} \quad \text{inverse Radon transform} \\ &= \beta \mathcal{H}\{\overbrace{\mathcal{R}[f(x, y)]}^{\substack{\text{backprojection} \\ \text{operator}}} \} \quad \text{Radon transform} \Rightarrow \text{projection} \\ &= \mathcal{R}^{-1}\{\mathcal{R}[f(x, y)]\} \quad \text{filtering the projection}\end{aligned}$$

where

$$\mathcal{H}\{p_\phi(x')\} = \mathcal{F}_1^{-1}[|\omega|] * p_\phi(x')$$

The inverse Radon transform can be represented as a filtering process followed by a back-projection operation.

Simple and Filtered Back-projection

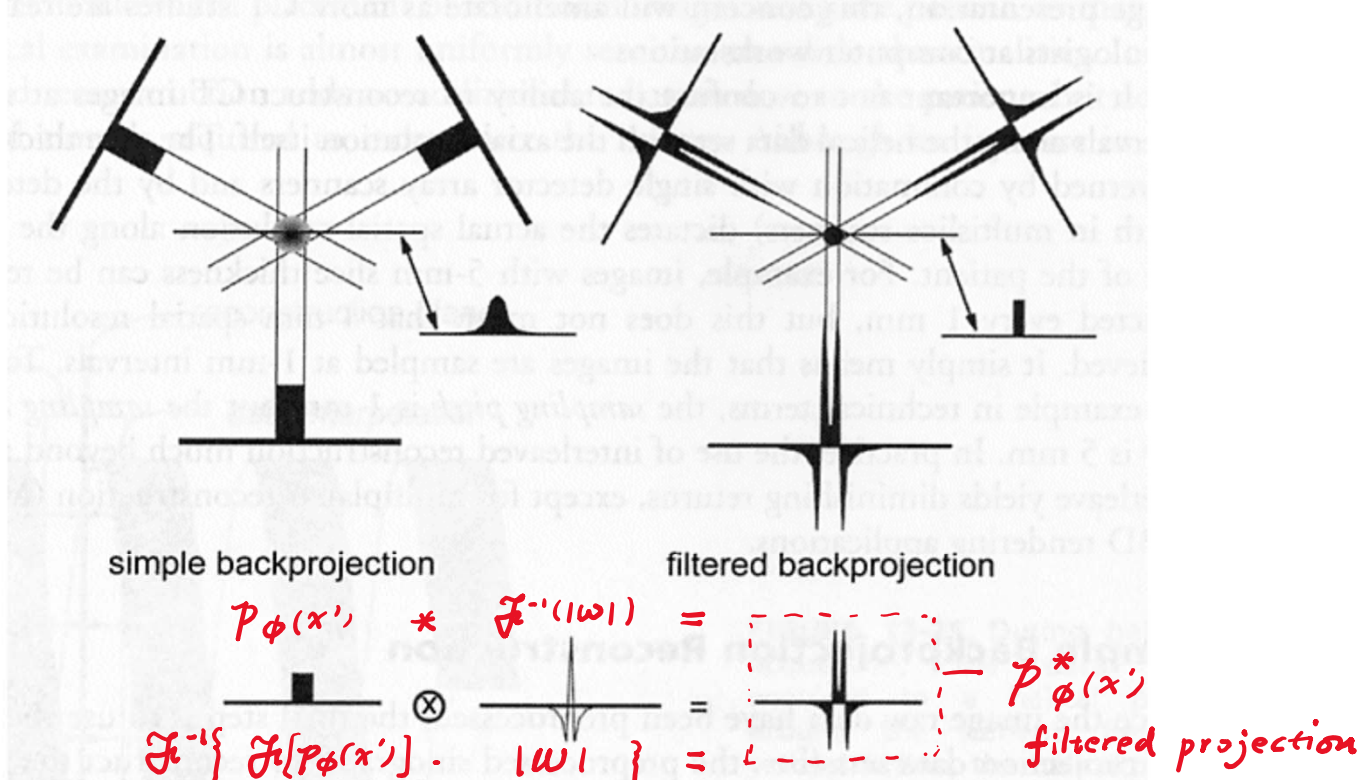
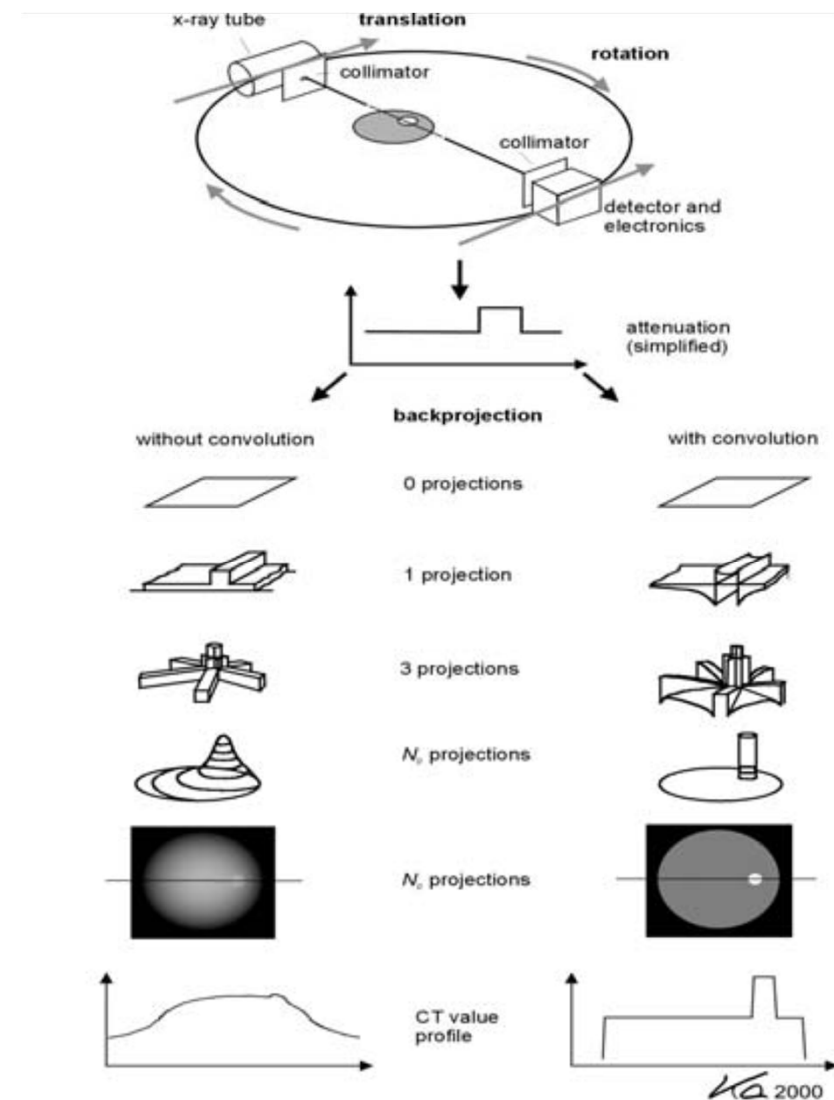


FIGURE 13-28. Simple backprojection is shown on the left; only three views are illustrated, but many views are actually used in computed tomography. A profile through the circular object, derived from simple backprojection, shows a characteristic $1/r$ blurring. With filtered backprojection, the raw projection data are convolved with a convolution kernel and the resulting projection data are used in the backprojection process. When this approach is used, the profile through the circular object demonstrates the crisp edges of the cylinder, which accurately reflects the object being scanned.

Chapters 12 & 13, The Essential Physics of Medical Imaging, Bushberg

Simple and Filtered Back-projection



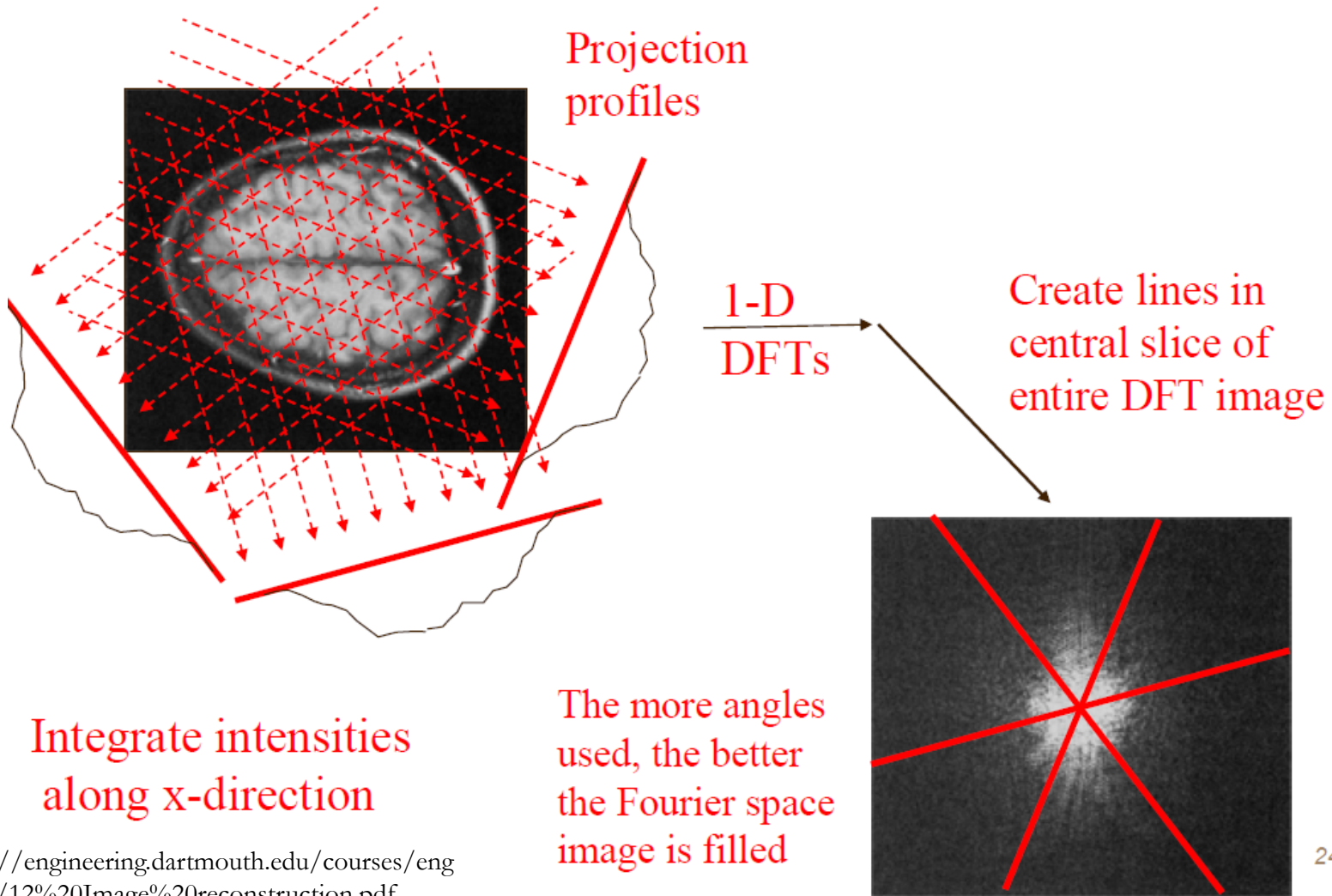
From Computed Tomography, Kalender, 2000.



Filtered Backprojection (FBP),

What and why?

Central Slice Theorem



One would need to use filter to compensate for this effect.

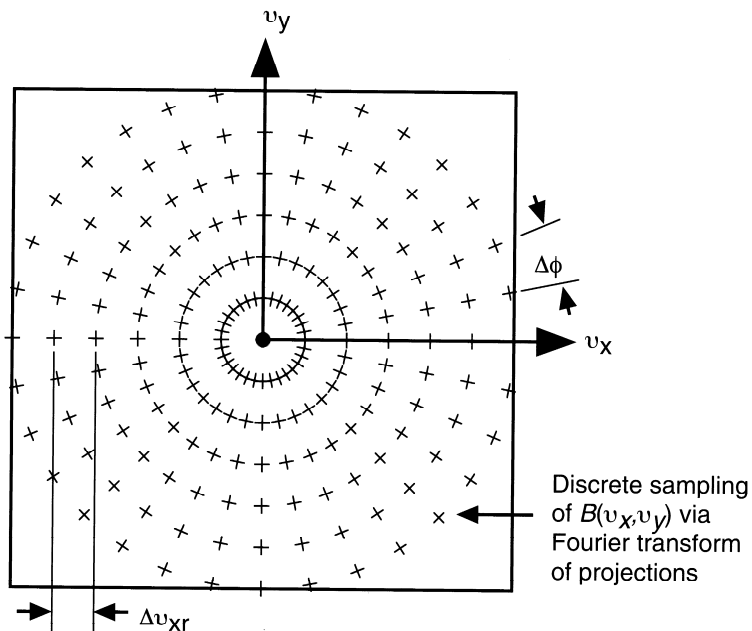


FIGURE 18 The discrete sampling pattern of $F(v_x, v_y)$ contained in $B(v_x, v_y)$, resulting from the use of discretely sampled projections.



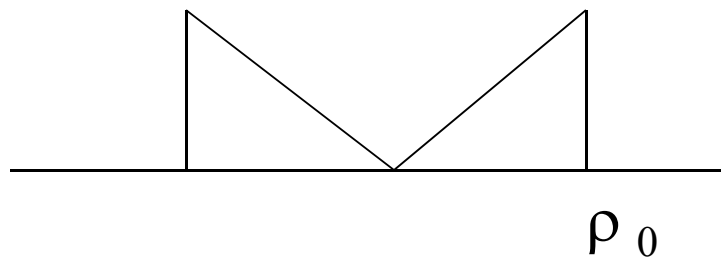
**Ideally, one would use a perfect filter as in the
Inverse Radon Transform**

Filtered Back-projection

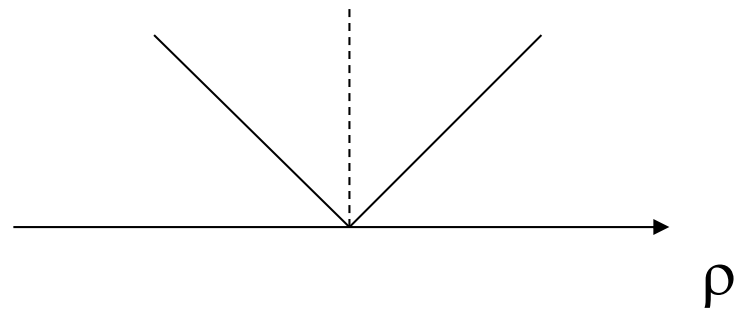
The Ram-Lak filter

$$H_{\text{RL}}(\omega) = \begin{cases} |\omega|, & (|\omega| \leq 2\pi B) \\ 0, & (\text{otherwise}) \end{cases}$$

Ram-Lak filter



Ideal filter





**Consider the bandwidth-limited nature of
most projection data, we have ...**

Filtered Back-projection

The Ram-Lak filter in spatial domain

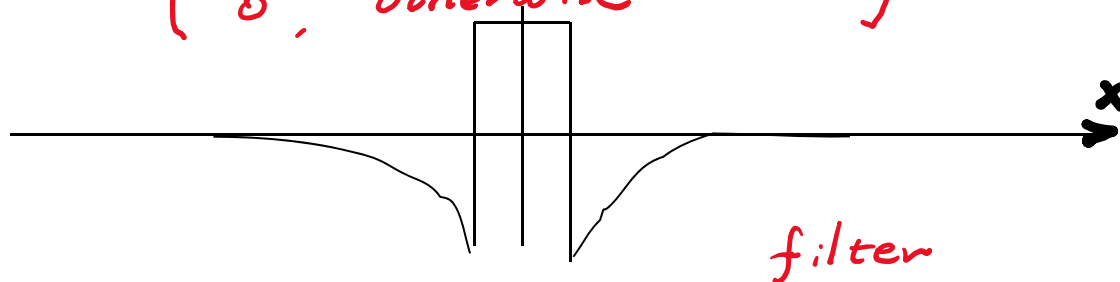
$$\rightarrow h_{RL}(x) = \frac{1}{2\pi} \int_{-\infty}^{\infty} H_{RL}(\omega) \exp(ix\omega) d\omega$$

$$= \frac{1}{2\pi} \int_{-2\pi B}^{2\pi B} |\omega| \exp(ix\omega) d\omega$$

$$= 2B^2 \text{sinc}(2\pi Bx) - B^2 \text{sinc}^2(\pi Bx)$$

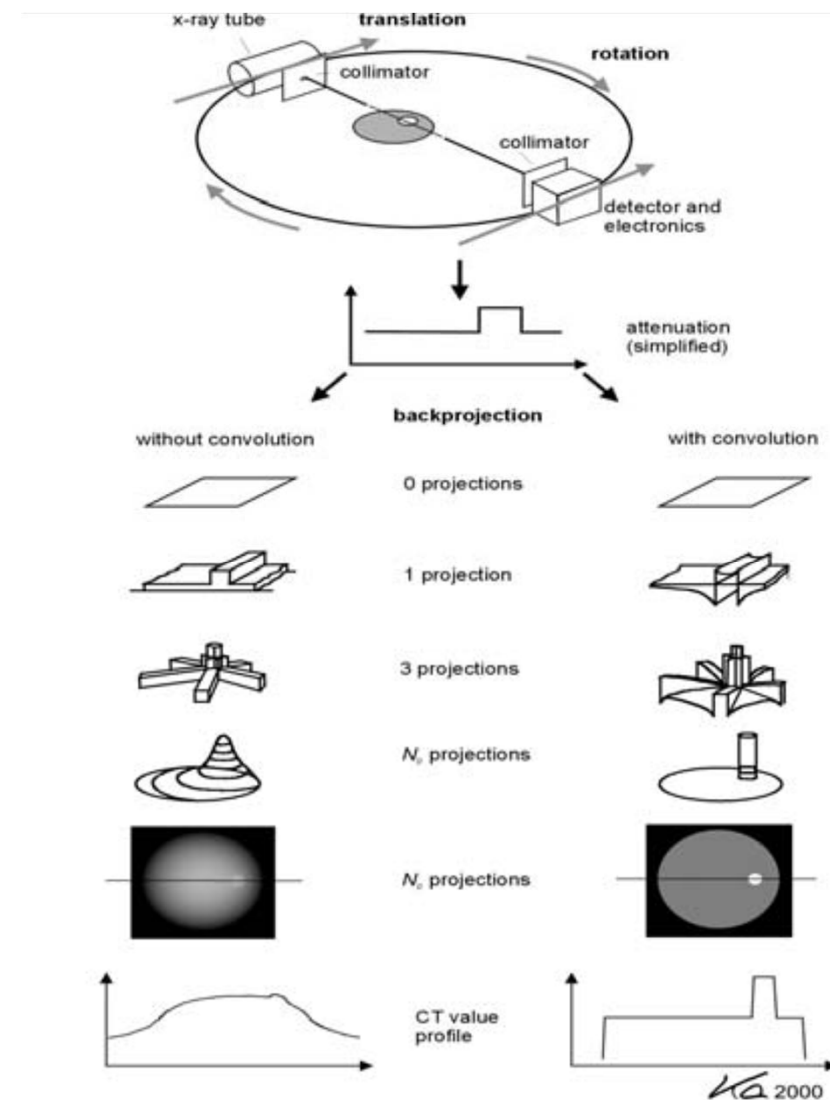
$$\rightarrow H_{RL} = \begin{cases} |\omega|, & |\omega| \leq 2\pi \cdot B \\ 0, & \text{otherwise} \end{cases}$$

$H_{RL}(\omega) = \mathcal{F}(h_{RL})$



$$p_{\phi}^*(x') = \int_{-\infty}^{\infty} dx' p_{\phi}(x') \underbrace{h(x \cos \phi + y \sin \phi - x')}$$

Simple and Filtered Back-projection



From Computed Tomography, Kalender, 2000.

Simple and Filtered Back-projection

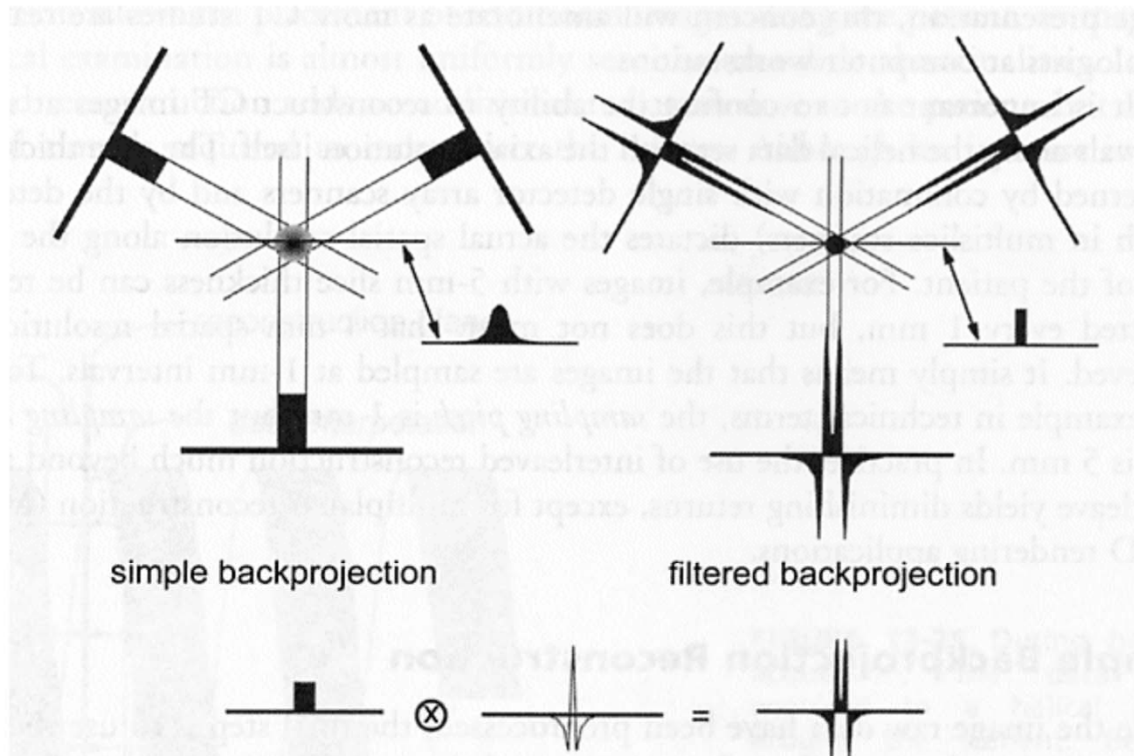
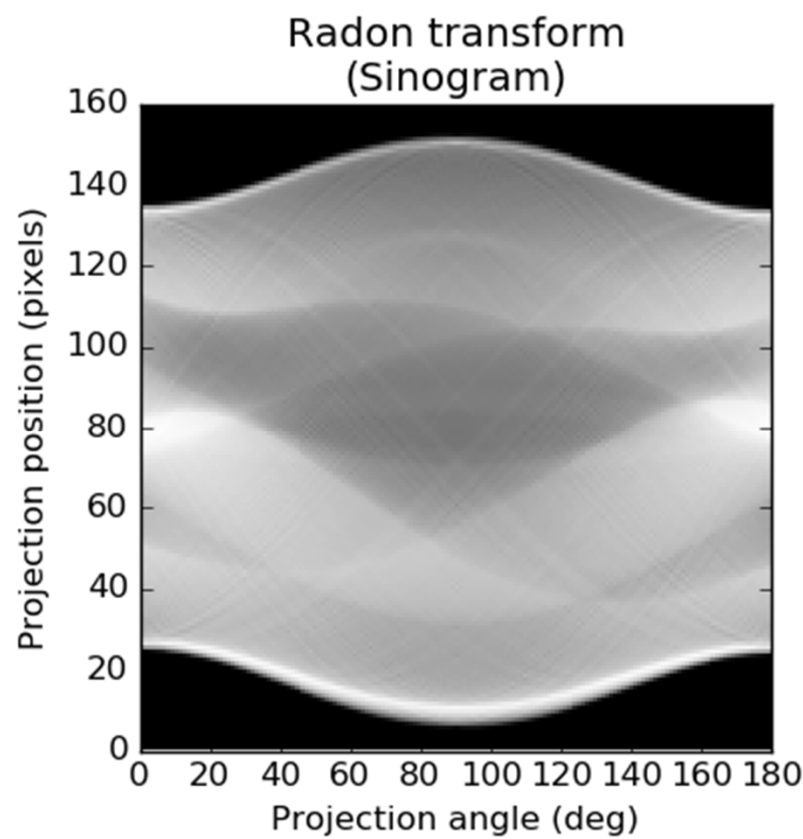
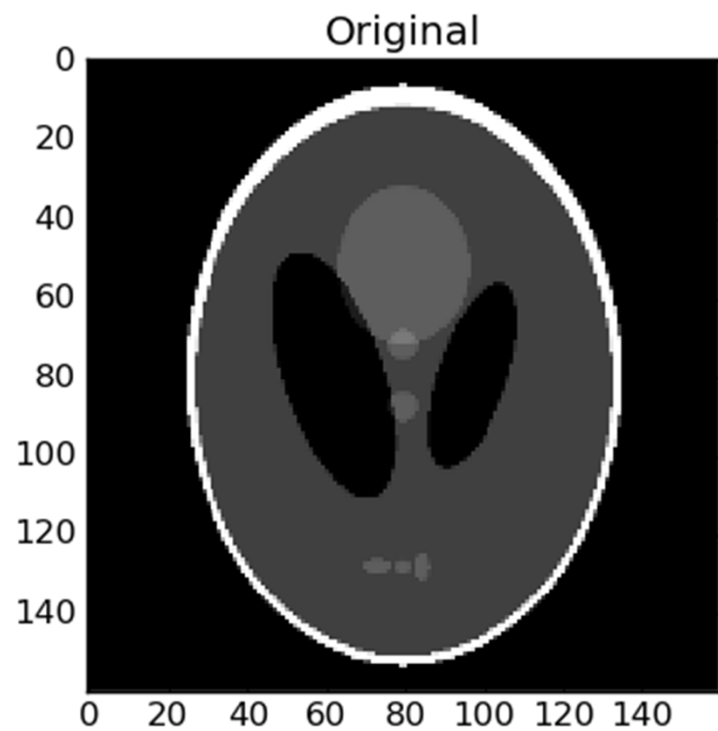


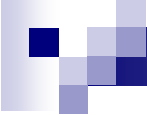
FIGURE 13-28. Simple backprojection is shown on the left; only three views are illustrated, but many views are actually used in computed tomography. A profile through the circular object, derived from simple backprojection, shows a characteristic $1/r$ blurring. With filtered backprojection, the raw projection data are convolved with a convolution kernel and the resulting projection data are used in the backprojection process. When this approach is used, the profile through the circular object demonstrates the crisp edges of the cylinder, which accurately reflects the object being scanned.

Chapters 12 & 13, The Essential Physics of Medical Imaging, Bushberg

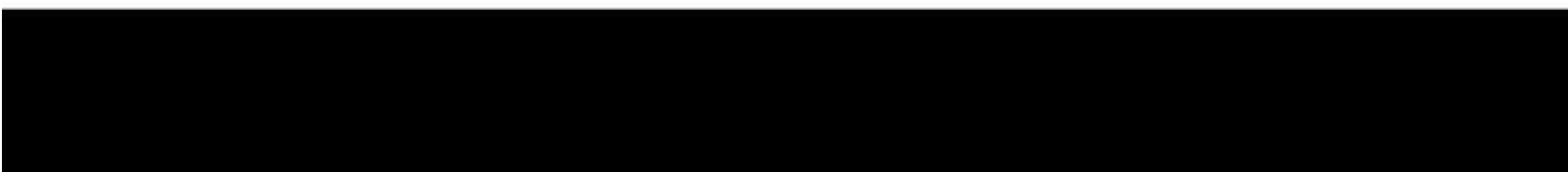
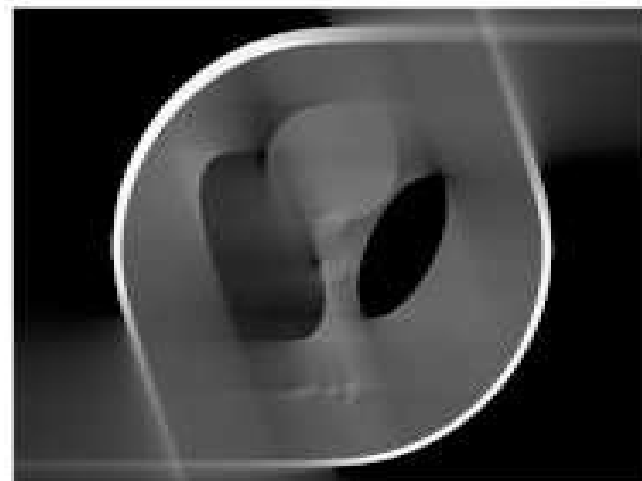
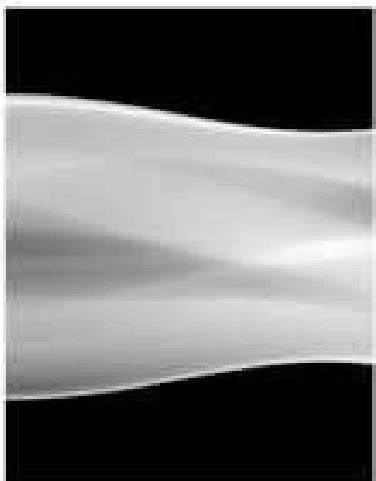
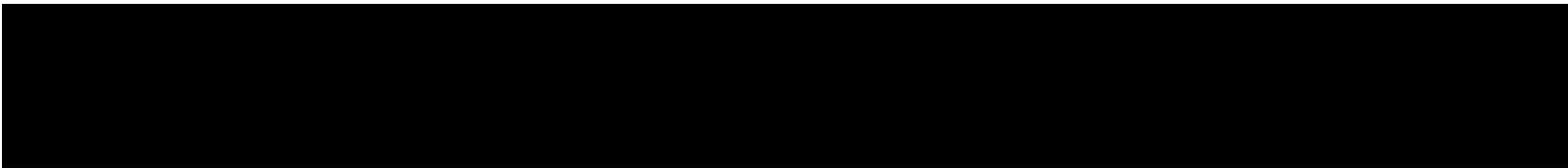
Radon Transform and Sinogram



<http://tech.snmjournals.org/cgi/content-nw/full/29/1/4/F3>



Filtered Back-projection



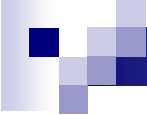
<https://www.youtube.com/watch?v=ddZeLNh9aac>



But is there something missing in this discussion?, such as

Noise in data?

Possible artifacts?



Filtered Back-projection – The Optimum Filter

Have we forgot something? What about the noise in the projection data?

Where is the noise coming from?

In reality, the true projection is

$$\dot{p}_\phi(x') = p_\phi(x') + n_\phi(x')$$

Review of Fourier Transform and Filtering Spectral Filtering

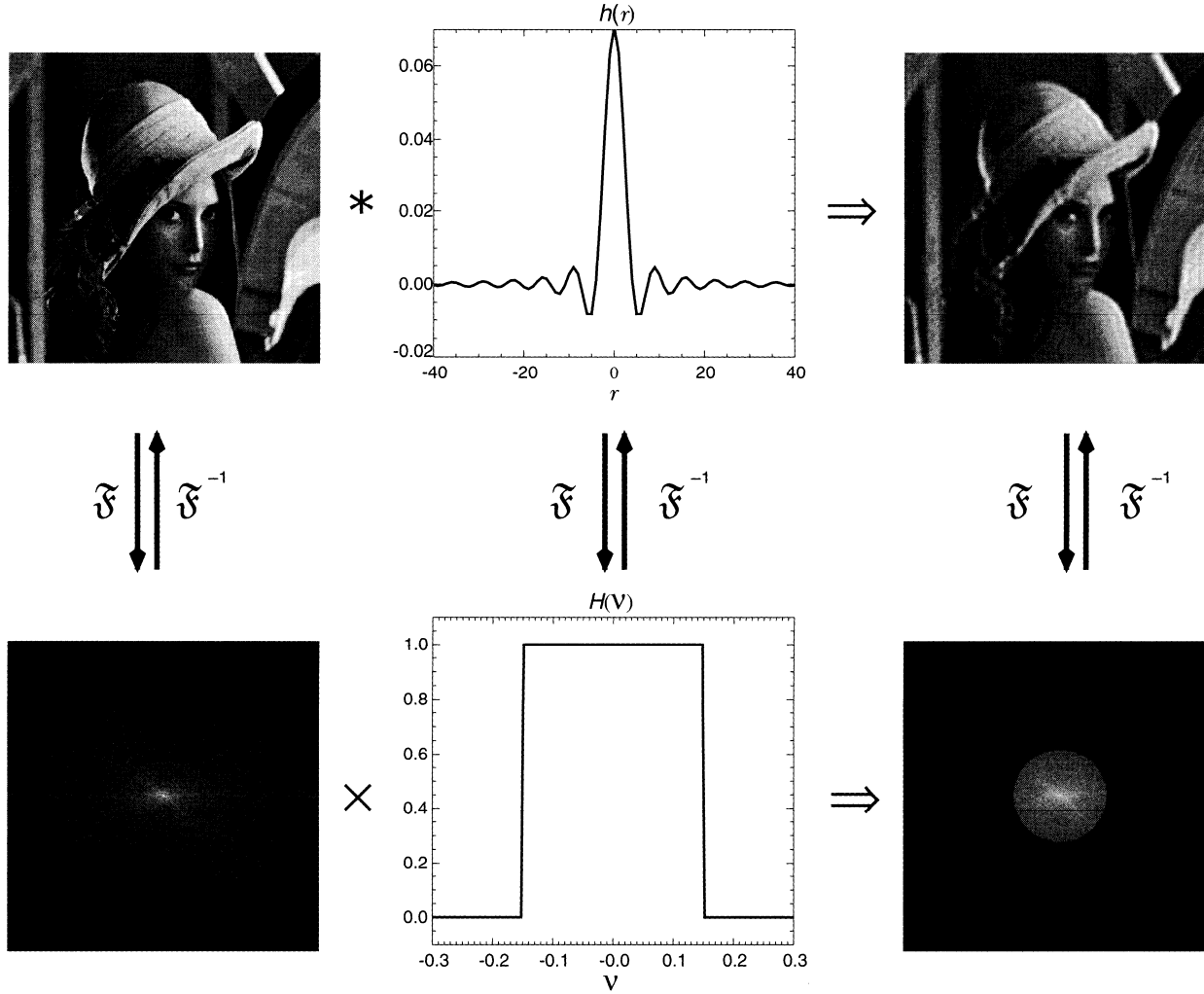


FIGURE 3 Ideal lowpass filtering of an image. Figures in the top and bottom rows demonstrate the filtering operation in the spatial and frequency domains, respectively. The left column shows the input image and the magnitude of its Fourier transform. The middle column are the circular symmetric PSF and its transfer function, where $v = \sqrt{v_x^2 + v_y^2}$ and $r = \sqrt{x^2 + y^2}$. Images in the right column are the output image and the magnitude of its Fourier transform.

Review of Fourier Transform and Filtering

Spectral Filtering

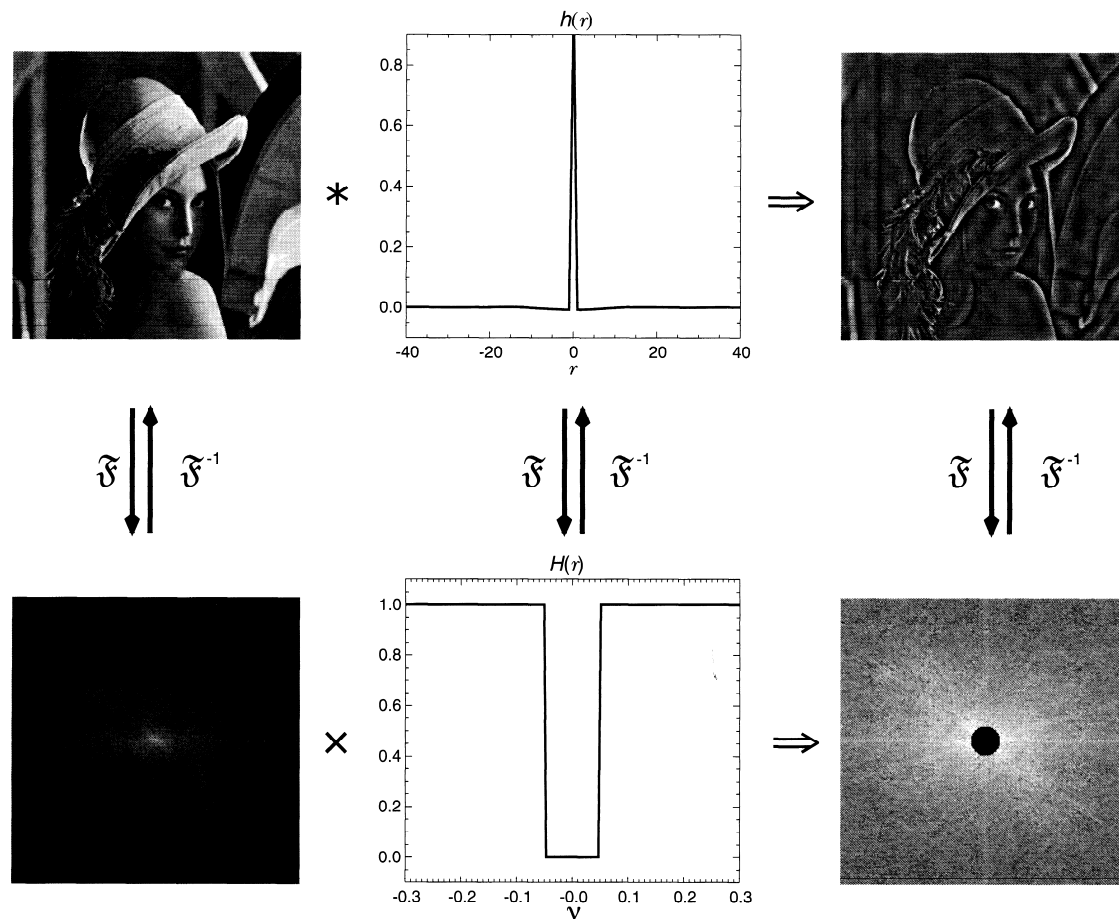
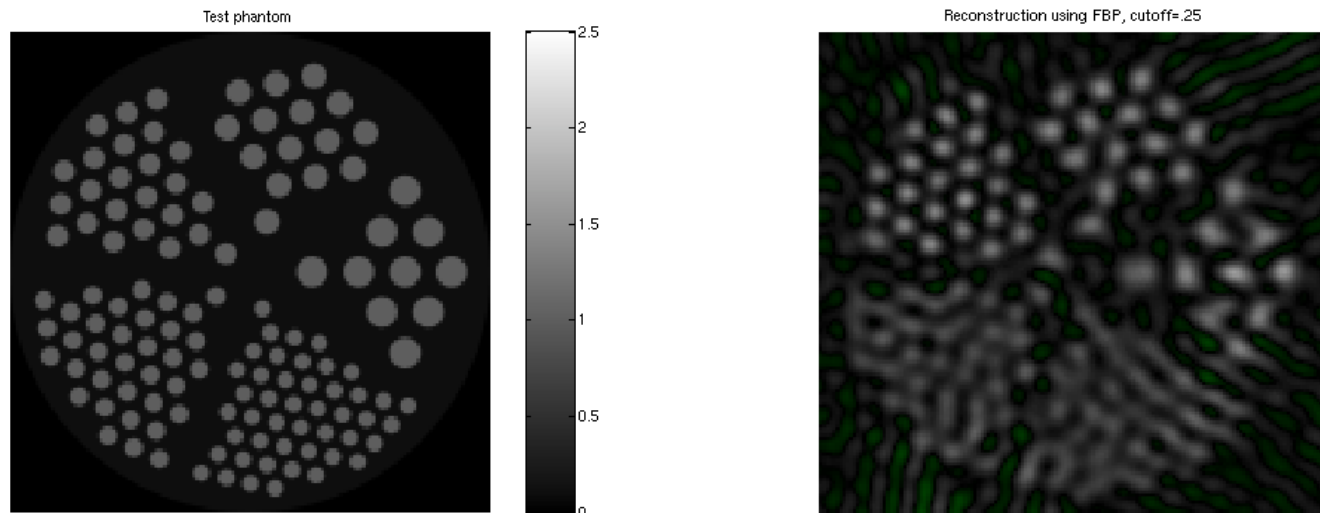


FIGURE 4 Ideal highpass filtering of an image. Figures in the top and bottom rows demonstrate the filtering operation in the spatial and frequency domains, respectively. The left column shows the input image and the magnitude of its Fourier transform. The middle column shows the circular symmetric PSF and its transfer function, where $v = \sqrt{V_x^2 + V_y^2}$ and $r = \sqrt{x^2 + y^2}$. Images in the right column are the output image and the magnitude of its Fourier transform.

Filtered Back-projection

The “ringing” artifacts in reconstructed images.

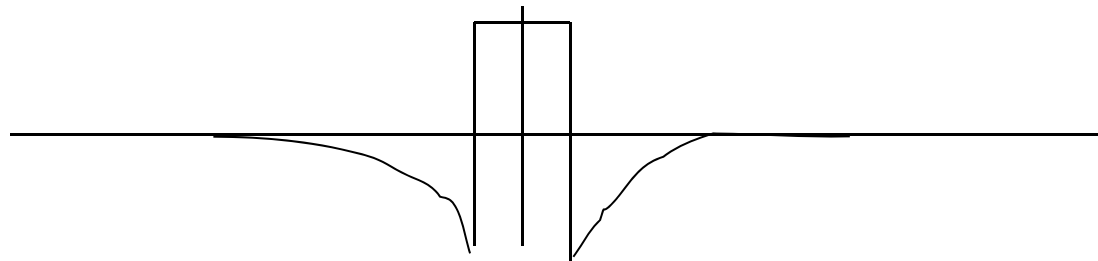


In this context it is usually manifest itself as "streak artifacts". You may, for example, see this as lines radiating from the center and outwards. The term comes from electronics and is meant in the sense of a bell-ringing.

Filtered Back-projection

The Ram-Lak filter in spatial domain

$$\begin{aligned} h_{\text{RL}}(x) &= \frac{1}{2\pi} \int_{-\infty}^{\infty} H_{\text{RL}}(\omega) \exp(ix\omega) d\omega \\ &= \frac{1}{2\pi} \int_{-2\pi B}^{2\pi B} |\omega| \exp(ix\omega) d\omega \\ &= 2B^2 \text{sinc}(2\pi Bx) - B^2 \text{sinc}^2(\pi Bx) \end{aligned}$$



$$\hat{f}(x, y) = \frac{1}{\pi} \int_0^\pi d\phi \int_{-\infty}^{\infty} dx' p_\phi(x') h(x \cos \phi + y \sin \phi - x')$$

Filtered Back-projection

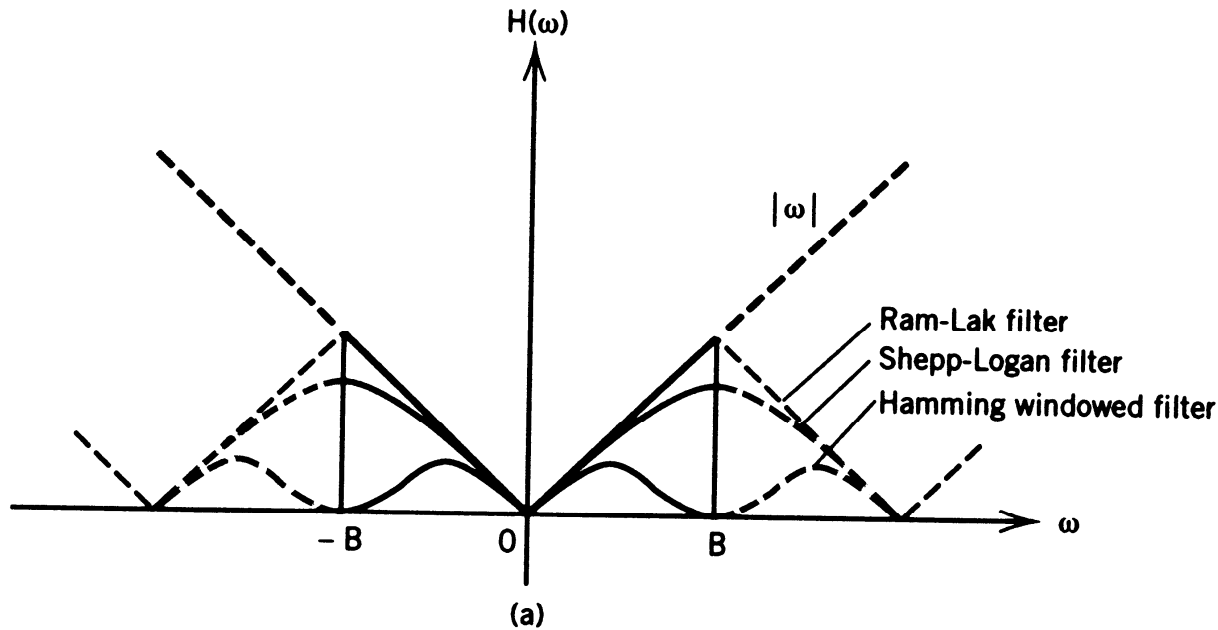


Figure 3-4 (a) Examples of the band-limited filter function of sampled data. Note the cyclic repetitiveness of the digital filter.

Filtered Back-Projection

$$\Delta x = 1/(2B),$$

Sampled version

$$h_{RL}(0) = B^2 = \frac{1}{4 \Delta x^2} \quad (\text{if } k = 0)$$

$$h_{RL}(k) = 0 \quad (\text{if } k \text{ even})$$

$$h_{RL}(k) = \frac{-4B^2}{\pi^2 k^2} = \frac{-1}{\pi^2 k^2 \Delta x^2} \quad (\text{if } k \text{ odd})$$

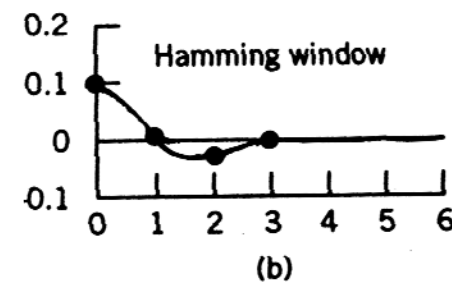
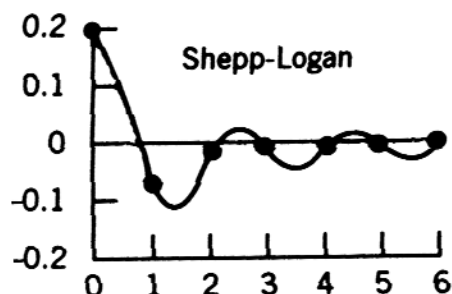
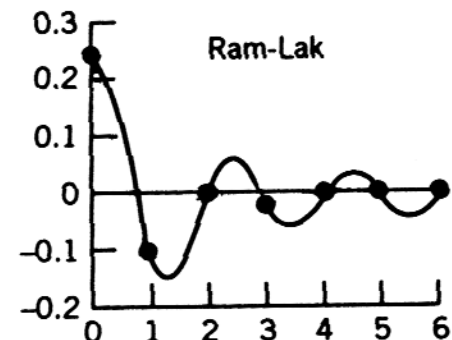


Figure 3-4 (b) Spatial domain filter kernels corresponding to the filter functions shown in the Ram-Lak filter is a high-pass filter with a sharp response but results in some noise enhancement, while the Shepp-Logan and the Hamming window filters are noise-smoothed filters and therefore have better SNR.

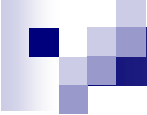
Filtered Back-projection

The sharp boundary of the Ram-Lak filter often make the spatial domain filter kernel oscillatory.

It sometime introduces the “ringing” artifacts in reconstructed images.
This can be effectively resolved by the Shepp and Logan filter

$$H_{SL}(\omega) = \begin{cases} |\omega| \sin\left(\frac{\omega}{4B}\right), & |\omega| < 2\pi B \\ 0, & \text{otherwise} \end{cases}$$

$$h_{SL}(x) = \frac{B}{\pi^2} \left\{ \frac{1 - \cos 2\pi B[(1/4B) + x]}{(1/4B) + x} + \frac{1 - \cos 2\pi B[(1/4B) - x]}{(1/4B) - x} \right\}$$



Filtered Back-projection

- Low spatial frequency data is overweighted. Filter to compensate for this. Weighted by $1/\rho$.
- Solution - filter each projection by $|\rho|$ to account for the uneven sampling density

Steps:

- 1) Projection operation
- 2) Transform projection
- 3) Weight with $|\rho|$
- 4) Inverse transform
- 5) Back project
- 6) Add all angles



**Any chance we can define an OPTIMUM
filter function for FBP?**

Filtered Back-projection

For FBP with noisy projection data, one can derive an optimum filter function. The FBP reconstruction has the minimum mean square error

$$M.S.E = E \left[(f(x,y) - \hat{f}(x,y))^2 \right]$$

In other words; there exists a filter function that can be used in the FBP reconstruction that produces the most faithful reproduction of the original image $f(x,y)$

Filtered Back-projection

For a situation in which we know the power spectra for both the image function $f(x,y)$ and the noise, the optimum filter function is

Where

$$H_{\text{opt}}(\omega, \phi) = |\omega| H_W(\omega, \phi)$$

Image degradation function

$$H_W(\omega, \phi) = \frac{H_D^*(\omega, \phi) W_P(\omega, \phi)}{|H_D(\omega, \phi)|^2 W_P(\omega, \phi) + W_{PN}(\omega, \phi)}$$

Signal power spectrum of the projection data at view angle ϕ

Power spectrum of the noise in the projection data at view angle ϕ

Remember that

$$W_p(\omega, \phi) = \left| \mathcal{F}[p_\phi(x')] \right|^2 = \left\{ \text{real} \left\{ \mathcal{F}[p_\phi(x')] \right\} \right\}^2 + \left\{ \text{imag} \left\{ \mathcal{F}[p_\phi(x')] \right\} \right\}^2$$

Fourier Transform

- In general, Fourier transform is a complex valued signal, even if $f(x,y)$ is real valued.
- It is sometimes useful to consider the ***magnitude*** and ***phase*** of the Fourier transform separately.

Fourier coefficients are complex:
$$F(u,v) = F_R(u,v) + j \cdot F_I(u,v)$$

Magnitude:
$$|F(u,v)| = \sqrt{F_R^2(u,v) + F_I^2(u,v)}$$

Phase:
$$\angle F(u,v) = \tan^{-1} \frac{F_I(u,v)}{F_R(u,v)}$$

An alternative representation:
$$F(u,v) = |F(u,v)| e^{j\angle F(u,v)}$$

- The square of the magnitude $|F(u,v)|^2$ is referred to as the ***power spectrum*** of the original function.

Filtered Back-projection with Optimum Filter

The optimum filter function can also be written as

$$H_W(\omega, \phi) = \frac{H_D^*(\omega, \phi)}{|H_D(\omega, \phi)|^2 + (W_{PN}(\omega, \phi)/W_P(\omega, \phi))}$$

And then

$$\begin{aligned} H_{\text{opt}}(\omega, \phi) &= |\omega| H_W(\omega, \phi) \\ &= \frac{|\omega| H_D^*(\omega, \phi)}{|H_D(\omega, \phi)|^2 + 1/\text{SNR}(\omega, \phi)} \end{aligned}$$

where $[W_P(\omega, \phi)]/[W_{PN}(\omega, \phi)]$ is the signal-to-noise ratio (**SNR**) of the projection data at a given view angle ϕ .

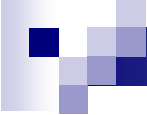
Filtered Back-projection

Therefore the optimum estimator (the optimum reconstruction) of the original image function $f(x,y)$ is

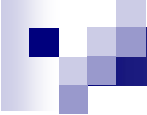
$$\hat{f}(x, y) = \frac{1}{\pi} \int_0^\pi d\phi \int_{-\infty}^{\infty} dx' \dot{p}_\phi^*(x') h(x \cos \phi + y \sin \phi - x')$$

where the filtered projection data is given by

$$\mathcal{F}_1^{-1} [H_{\text{opt}}(\omega, \phi)] * \dot{p}_\phi(x') = \dot{p}_\phi^*(x').$$



Most of current X-ray CT work in
fan-beam mode ...



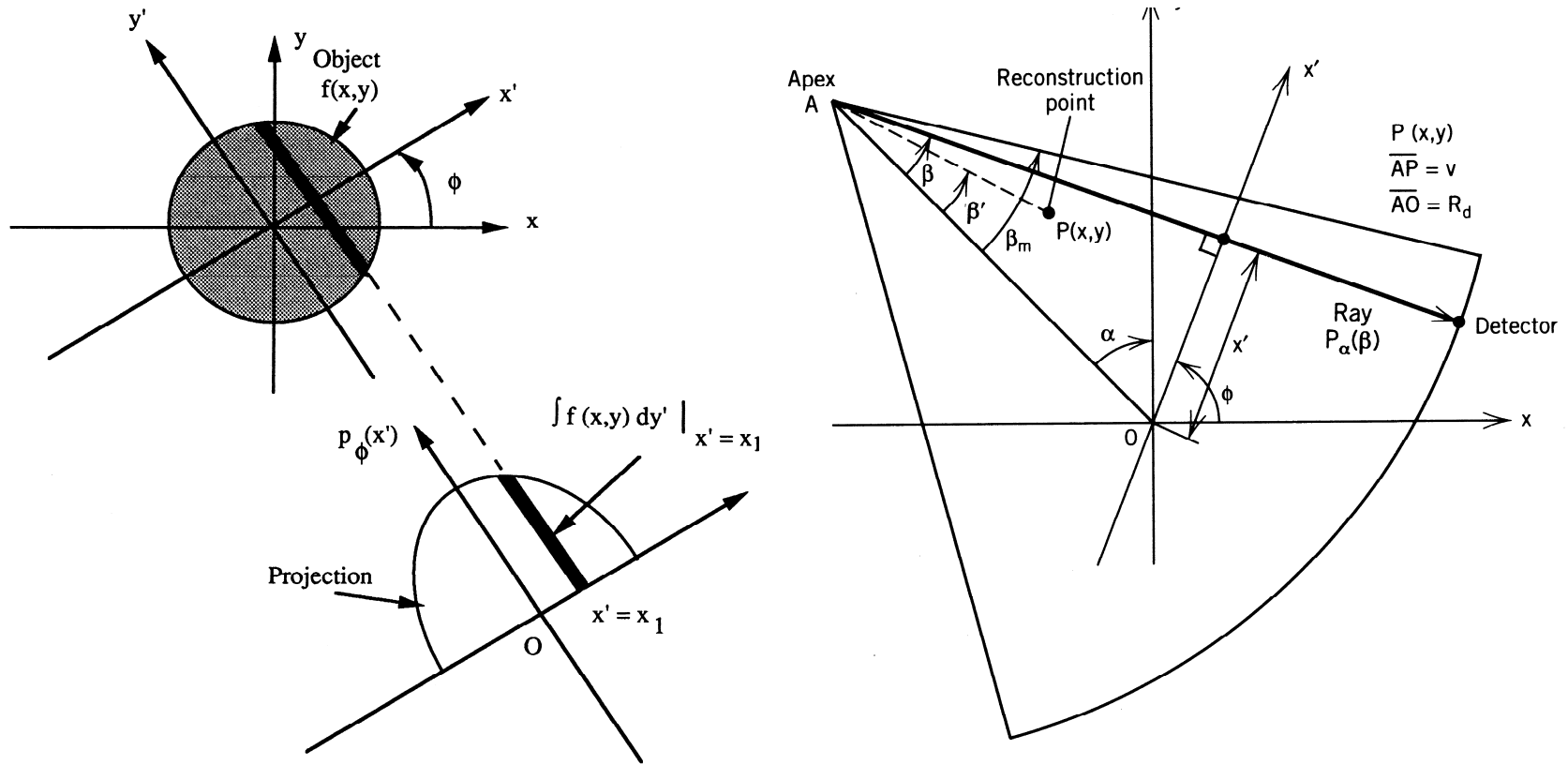
Filtered Back-projection in Fan-beam Mode

Why fan beam mode?

Most modern X-ray CT system use fan (or cone) beam data acquisition scheme.

Image reconstruction with fan beam mode often provide better spatial resolution with the same dimension of sampled data as the parallel case, due to the improved sampling at the central region. This is found to be important for PET, where the intrinsic limitation on spatial resolution is on the finite detector size.

Filtered Back-projection in Fan-beam Mode



Comparing parallel beam and fan beam geometries

Filtered Back-projection in Fan-beam Mode

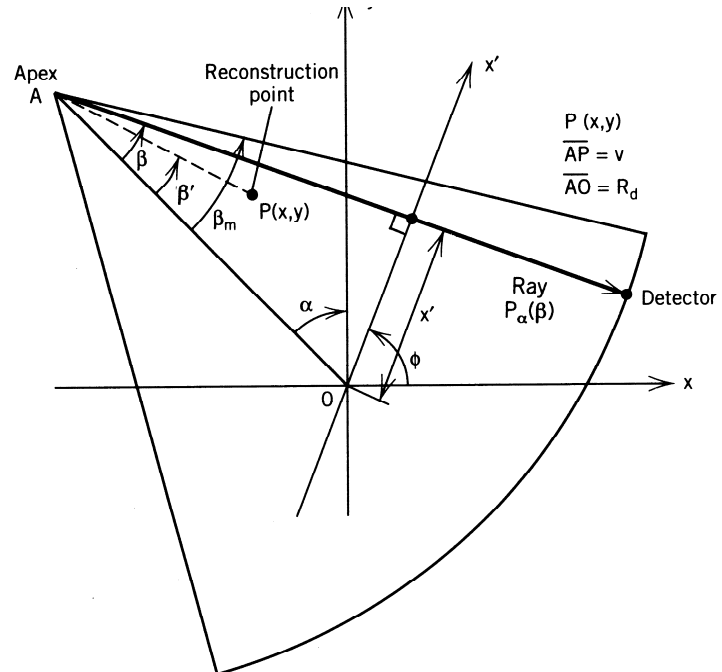
where β' is the angle between central line and the line passing through the reconstructed point at (x,y) . And v is the distance between the apex of fan and the reconstruction point p .

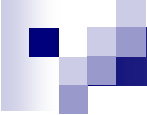
$$v = \sqrt{(x \cos \alpha + y \sin \alpha)^2 + (x \sin \alpha - y \cos \alpha + R_d)^2}$$

$$\beta' = \tan^{-1} \left[\frac{x \cos \alpha + y \sin \alpha}{x \sin \alpha - y \cos \alpha + R_d} \right]$$

$$x' = R_d \sin \beta$$

$$\phi = \alpha + \beta$$





Filtered Back-projection in Fan-beam Mode

The basic idea:

The mathematical treatment for fan beam mode is almost identical to that for parallel beam case with changing parameters!

Starting from the one-to-one relationship between the parallel beam projection space (ϕ, x') and fan beam projection space (α, β),

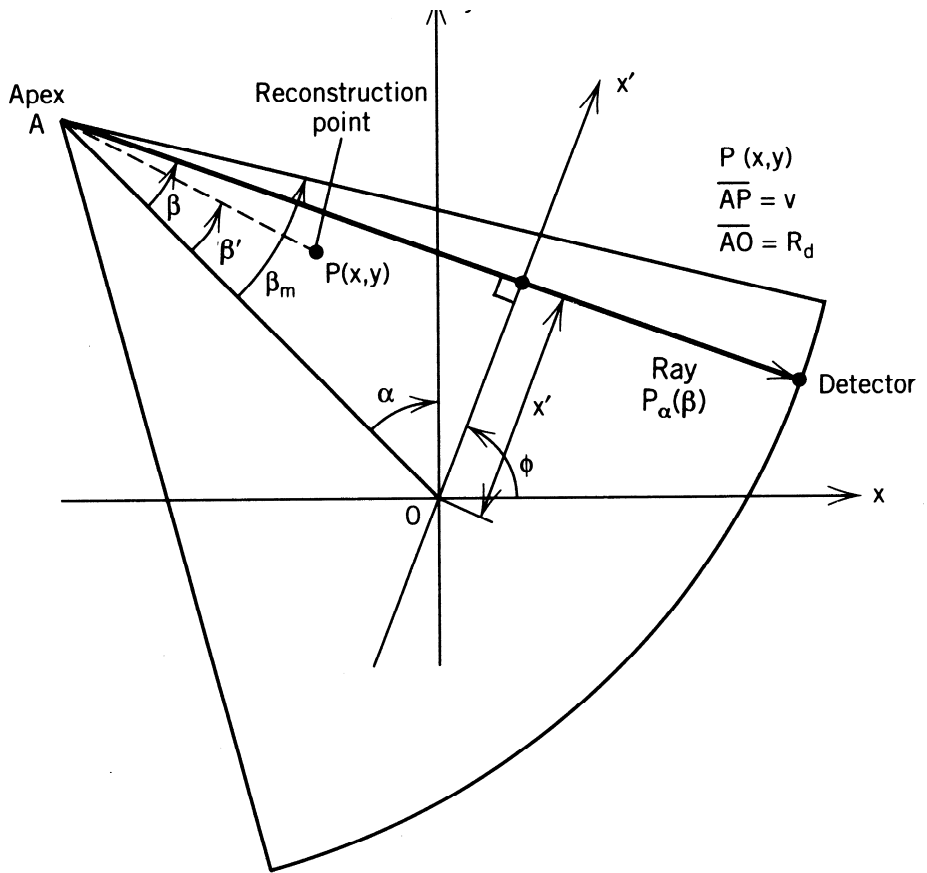
$$x' = R_d \sin \beta$$

$$\phi = \alpha + \beta$$

Filtered Back-projection in Fan-beam Mode

$$x' = R_d \sin \beta$$

$$\phi = \alpha + \beta$$



Where the Jacobian $|J|$ is

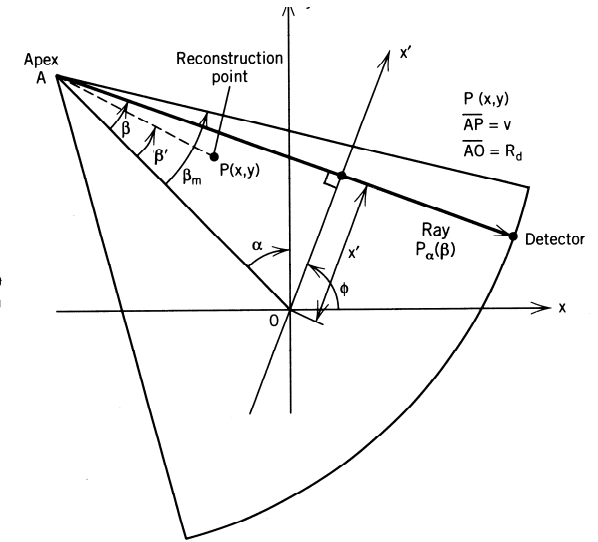
$$|J| = \left| \frac{\partial(x', \phi)}{\partial(\alpha, \beta)} \right| = R_d \cos \beta$$

Filtered Back-projection in Fan-beam Mode

Where the Jacobian $|J|$ is

$$|J| = \left| \frac{\partial(x', \phi)}{\partial(\alpha, \beta)} \right| = R_d \cos \beta$$

and the FBP in fan beam mode becomes

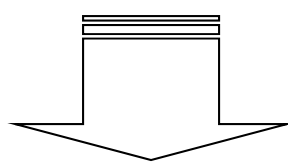


$$\hat{f}(x, y) = \frac{1}{2\pi} \int_0^{2\pi} d\alpha \int_{-\beta_m}^{\beta_m} d\beta p_\alpha(\beta) h\{v \sin(\beta' - \beta)\} |J|$$

Filter Function in Fan-beam Mode

Similarly the filter function used in fan beam mode is a direct transformation from the parallel beam counterpart

$$\begin{aligned} h(x) &= \mathcal{F}_1^{-1}[|\omega|] \\ &= \mathcal{F}_1^{-1}[H(\omega)] \end{aligned}$$



$$x' = R_d \sin \beta$$

$$\phi = \alpha + \beta$$

$$h\{v \sin(\beta' - \beta)\} = \frac{1}{2\pi} \int_{-\infty}^{\infty} d\omega |\omega| \exp[i\omega v \sin(\beta' - \beta)]$$

Filtered Back-projection in Fan-beam Mode

FBP in parallel beam case

$$\hat{f}(x, y) = \frac{1}{2\pi} \int_0^{2\pi} d\phi \int_{-\infty}^{\infty} dx' p_\phi(x') h(x \cos \phi + y \sin \phi - x')$$

$$x' = R_d \sin \beta$$

$$\phi = \alpha + \beta$$

can be converted to FBP in fan beam mode by changing integration variables

$$\begin{aligned} \hat{f}(x, y) &= \frac{1}{2\pi} \int_0^{2\pi} d\alpha \int_{-\beta_m}^{\beta_m} d\beta \\ &\times p_\alpha(\beta) h\{x \cos(\alpha + \beta) + y \sin(\alpha + \beta) - R_d \sin \beta\} |J| \end{aligned}$$

Filtered Back-projection in Fan-beam Mode

Where the Jacobian $|J|$ is

$$|J| = \left| \frac{\partial(x', \phi)}{\partial(\alpha, \beta)} \right| = R_d \cos \beta$$

and the FBP in fan beam mode becomes

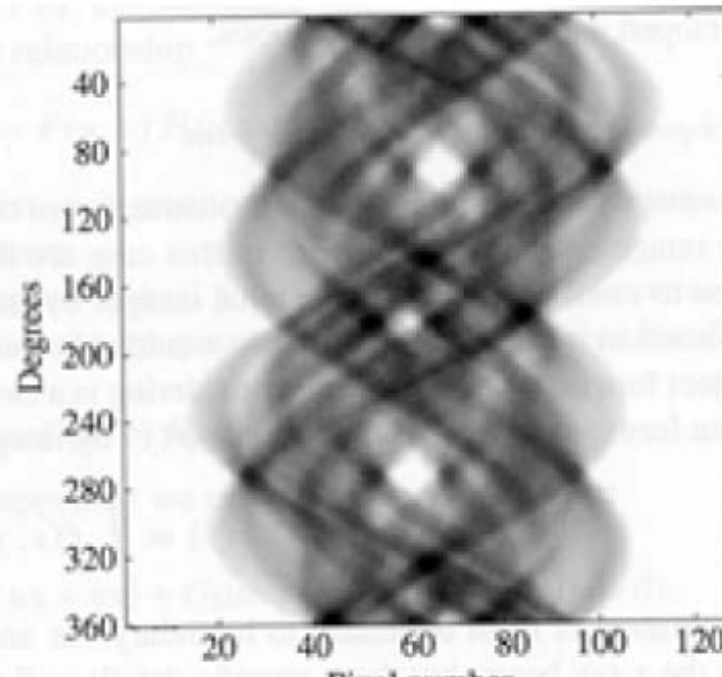
$$\hat{f}(x, y) = \frac{1}{2\pi} \int_0^{2\pi} d\alpha \int_{-\beta_m}^{\beta_m} d\beta p_\alpha(\beta) h\{v \sin(\beta' - \beta)\} |J|$$



Back-projection and Filtering Method for Reconstruction

Simple Back-projection and the $1/r$ Blurring

MP
BE



(a)

(b)

Figure 11.12. (a) An image and (b) the Radon projection or sinogram of this image. The wavy sine-like patterns explain the use of the term sinogram.

From Medical Physics and Biomedical Engineering, Brown, IoP Publishing

Simple Back-projection and the $1/r$ Blurring Revisited

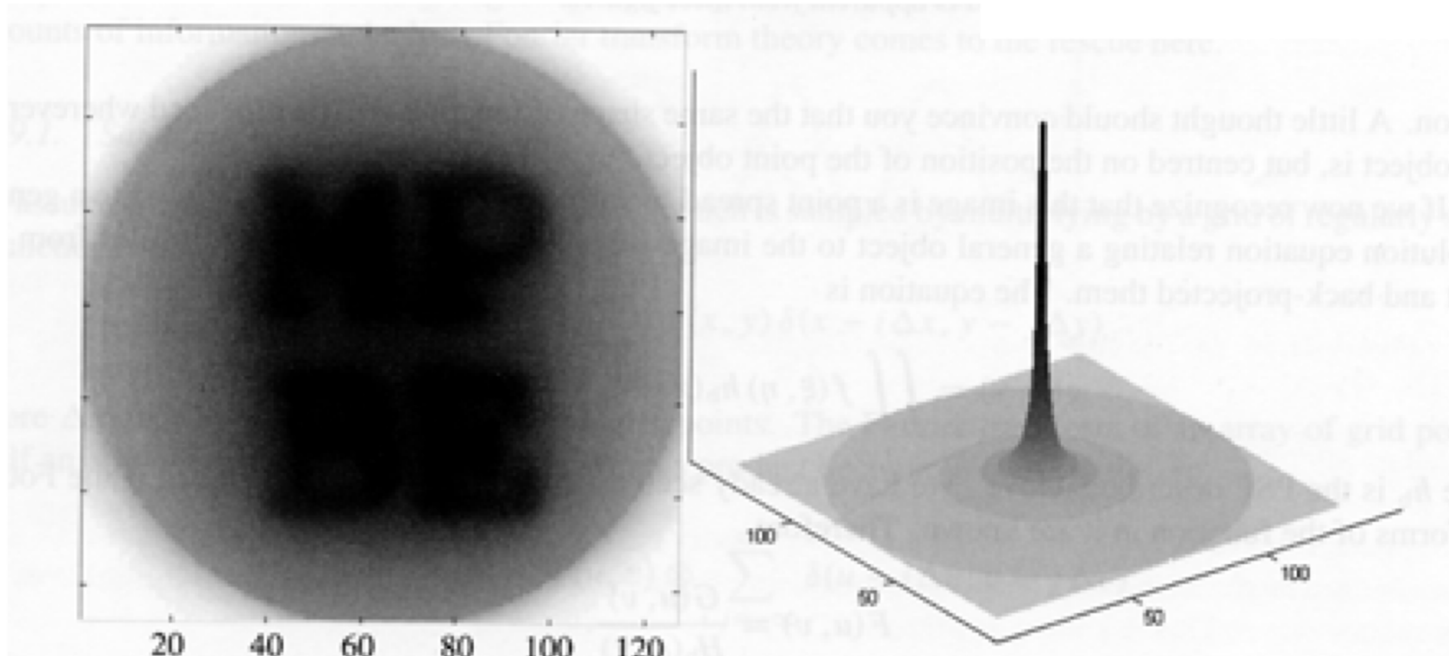
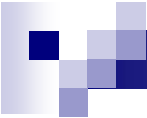


Figure 11.14. (a) Image produced by back-projecting the sinogram given in figure 11.12(b); (b) the response to a point object in the middle of the field of view.

From Medical Physics and Biomedical Engineering, Brown, IoP Publishing



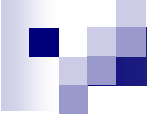
Impulse Response Function of Simple Backprojection Operator Revisited

$$h_b(r) = 1/r$$

$$f_b(x,y) = f(x,y) * 1/r$$

$$F_b(\rho, \phi) = F(\rho, \phi) / \rho \quad \text{since } F\{1/r\} = 1/\rho$$

Back projected image is blurred by convolution with $1/r$



Reconstruction with Back-projection and Filtering

If we know that the consequence of simple back-projection (under certain assumptions) is to apply a $1/r$ blurring on the input image ...

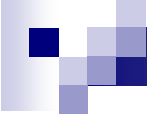
$$b(x, y) = f(x, y) * * \left(\frac{1}{r} \right)$$

Can we envisage an alternative reconstruction method that

Back projection first

and then

De-convolve the $1/r$ blurring?



Reconstruction with Back-projection and Filtering

The scheme leads to the back-projection and filtering reconstruction method

$$\hat{f}(x, y) = \mathcal{F}_2^{-1}[\rho B(\omega_x, \omega_y)]$$

where ρ is the radial spatial frequency and

$$B(\omega_x, \omega_y) = \mathcal{F}_2[b(x, y)]$$

Simple Backprojection --BB

Crude Idea 1: Take each projection and smear it back along the lines of integration it was calculated over.

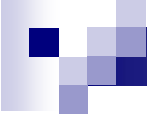
Result from a back projection from a single view angle:

$$b_\phi(x, y) = \int p(\phi, x') \delta(x \cos \phi + y \sin \phi - x') dx'$$

Adding up all the back projections from all the angles gives,

$$f_{\text{back-projected}}(x, y) = \int b_\phi(x, y) d\phi$$

$$B(x, y) = f_b(x, y) = \int_0^\pi d\phi \int_{-\infty}^{\infty} p(\phi, x') \delta(x \cos \phi + y \sin \phi - x') dx'$$

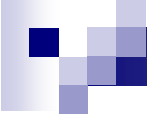


Reconstruction with Back-projection and Filtering

BPF reconstruction provides relatively poor images compared with FBP results because of the following two issues:

The back projection step results in an image with infinite extend. Cutting it to $N \times N$ points for filtering leads to loss of information.

The 2-D filter function discussed above has a slope discontinuity and therefore leads to ringing artifact.



Reconstruction with Back-projection and Filtering

If high quality reconstructions were to be achieved the BPF method, the following aspects have to be considered

Although the final reconstruction is on $N \times N$ points, the back projection step should use an matrix that is at least $2N \times 2N$.

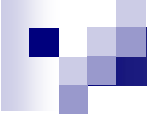
We would need to apply appropriate windowing to the filter function discussed above, just like in the parallel beam case ...

Reconstruction with Back-projection and Filtering

The procedures of BPF algorithm is VERY SIMPLE!

1. Obtain the backprojected image at least up to $2N \times 2N$ if the size of the original image matrix is $N \times N$.
2. Obtain the 2-D FFT of the full $2N \times 2N$ data array.
3. Obtain the optimum filtering in 2-D in Fourier domain by multiplication of ρ filter.
4. Obtain the 2-D inverse FFT and select the $N \times N$ image in the central region.
5. Normalize the image.

From Page 88, Foundation of Medical Imaging, Z. H. Cho, John Wiley & Sons, 1993.



Review of 2-D Analytical Reconstruction Methods

Key concepts:

Mathematical framework for modeling the projection process

- Radon transform
- Central slice theorem

Characteristics of typical projection data

- Non-uniform sampling of the 2-D Fourier transform space
- Actual measurements are associated with statistical noise and detector imperfections.

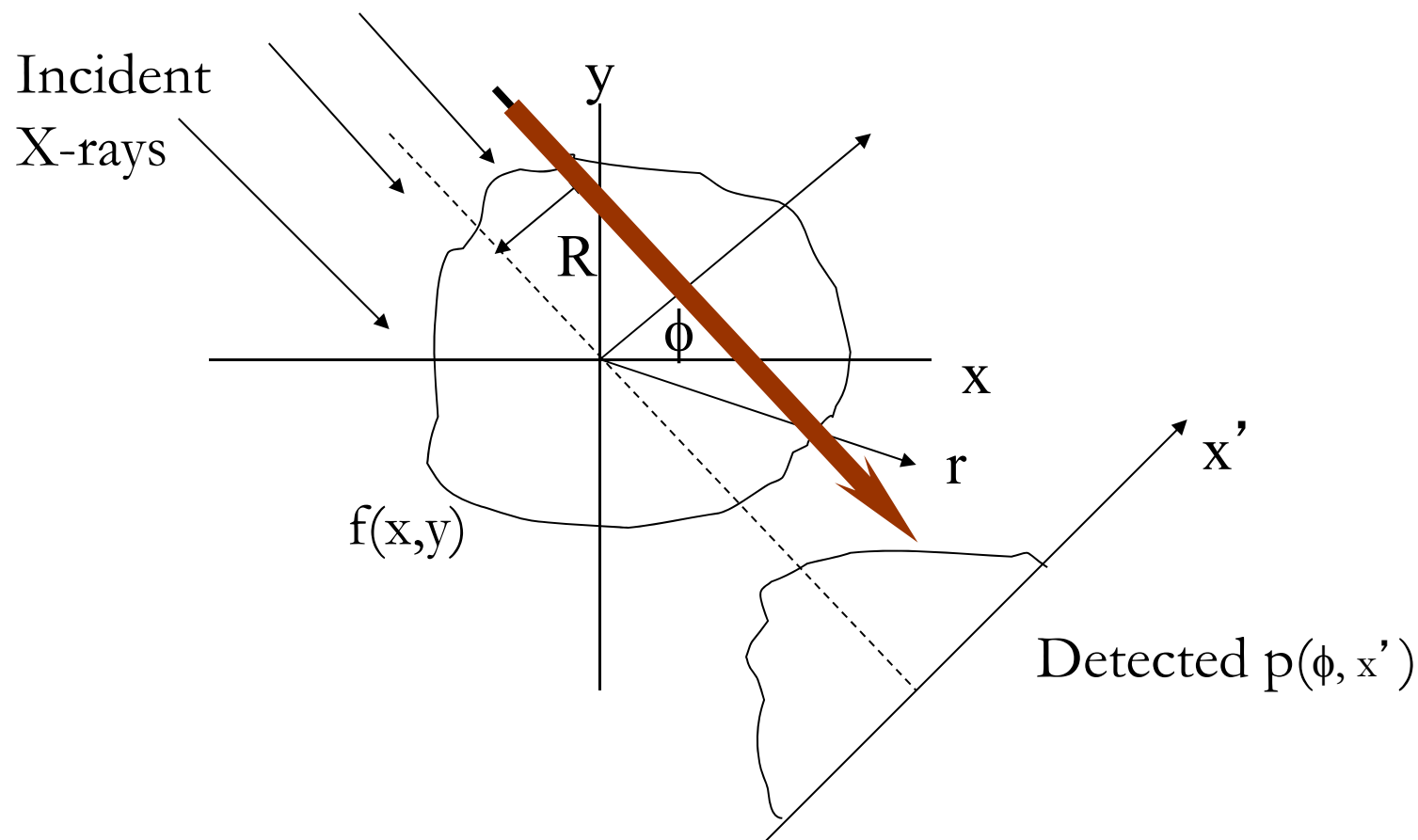
Analytical reconstruction methods

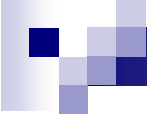
- Inverse Radon transform
- Filtered back-projection (FBP)
- FBP in fan-beam geometry
- Back-projection and filtering (BPF)

Review of 2-D Analytical Reconstruction Methods

Projection Data

Projection data $p(\phi, x')$





Review of 2-D Analytical Reconstruction Methods

Projection Data

Projection data are obtained as line-integrals from view different angles and radial distances from the center.

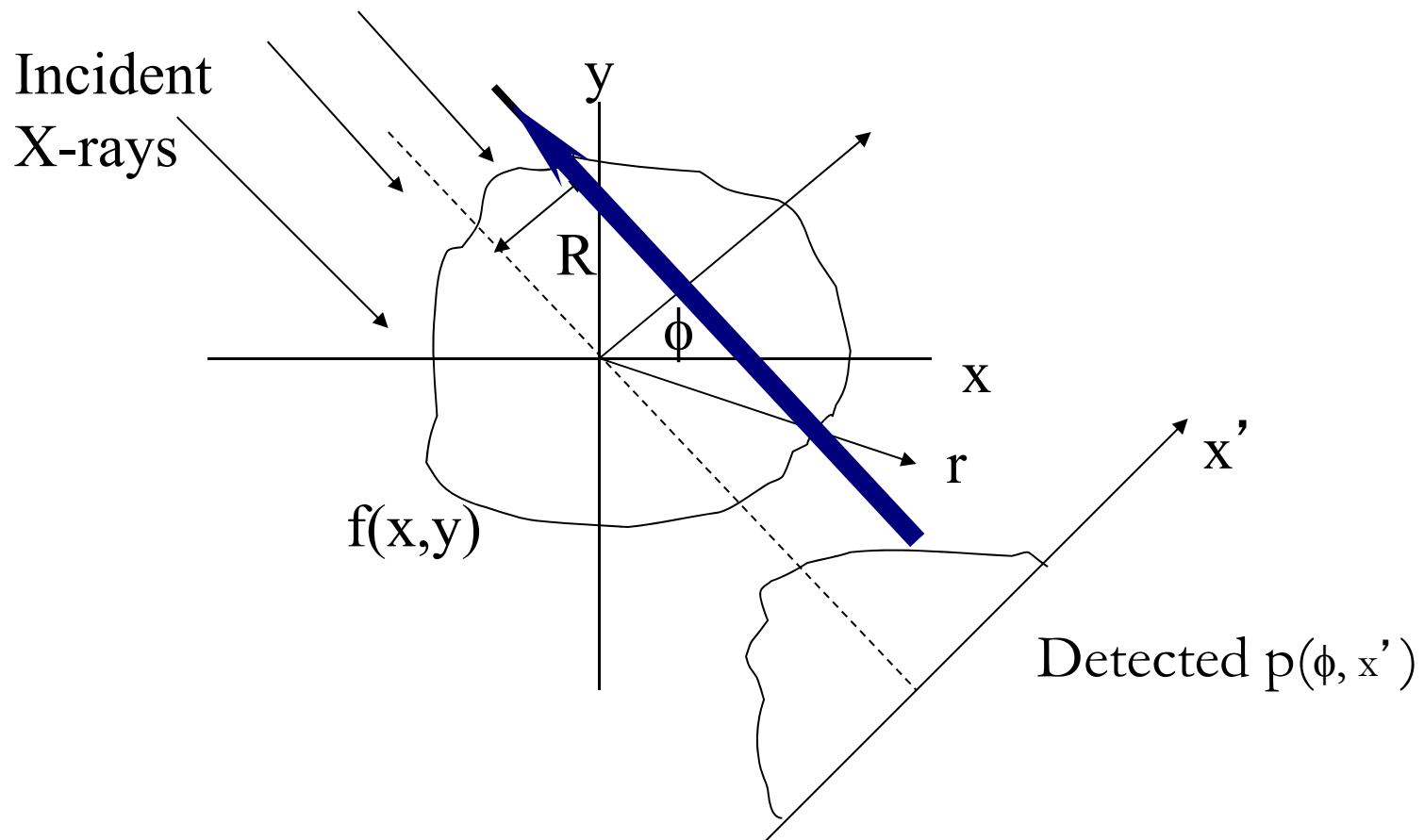
Projection data is a 2-D function representing the original function $f(x,y)$ transformed into the projection data space.

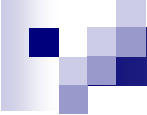
Given (a) a sufficiently sampling rate and (b) a band-limited image and (c) a perfect measurement, the projection data contains all information required to recover the original image.

Projection operation either through actual measurements or Radon transform, map 2-D function into the sinogram space.

Review of 2-D Analytical Reconstruction Methods

Back Projection Operation





Review of 2-D Analytical Reconstruction Methods

Projection Data

Back projection assign a constant value to each element along the projection lines (or lines of response, LOR). The value assigned is proportional to the projection function evaluated at the corresponding location on the x' axis.

Back projection is NOT an exact inverse operation of the projection due to the lack of the information regarding the actual distribution of the original function along the LOR.

Back projection does NOT provide an exact reproduction of the original function, $f(x,y)$. Instead, it provide an image that is the convolution of the original image with a $1/r$ blurring.

Review of 2-D Analytical Reconstruction Methods

Back Projection Operation

This $1/r$ blurring reveals an important aspect of the projection operation: The original function was *sampled non-uniformly* sampling rate across both (x,y) and (u,v) planes.

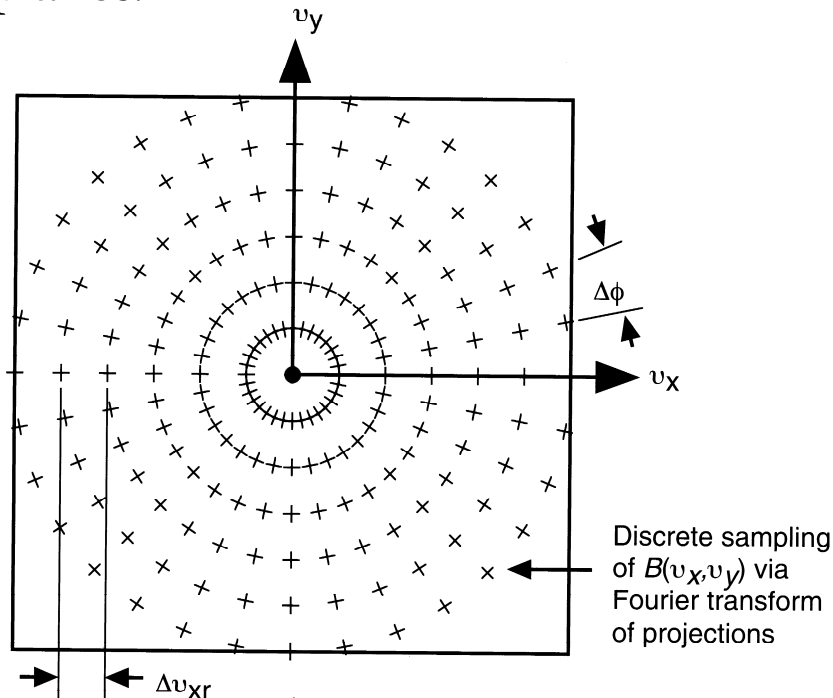
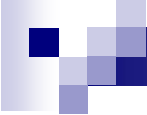


FIGURE 18 The discrete sampling pattern of $F(v_x, v_y)$ contained in $B(v_x, v_y)$, resulting from the use of discretely sampled projections.

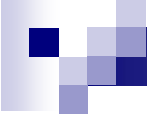


Review of 2-D Analytical Reconstruction Methods

Filtered Back Projection (FBP)

The basic idea of analytical reconstruction is to recover the original image (a) using back projection operation and (b) applying filters in either spatial frequency domain or spatial domain to compensate for the non-uniform sampling.

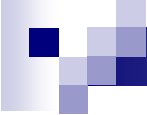
The approach of correcting for the non-uniform sampling in the projection data space and then performing back projection leads to the Filtered Back Projection (FBP) Method



Review of 2-D Analytical Reconstruction Methods

Back Projection and Filtering (BPF)

The approach performing back projection first and followed by the correction for the non-uniform sampling in the (x,y) space is called Back Projection and Filtered (BPF) Method



Review of 2-D Analytical Reconstruction Methods

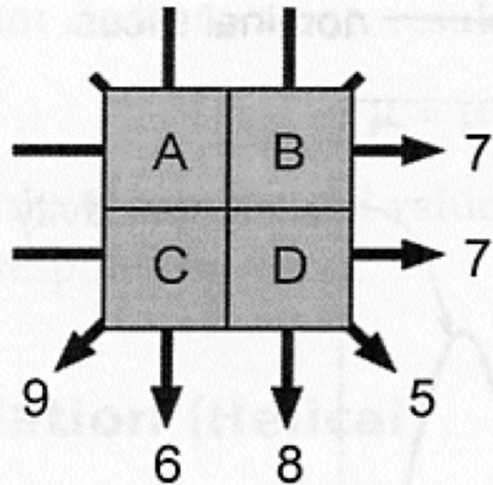
Filtered Back Projection

As a matter of fact, FBP provides almost optimum image quality with good quality projection data, but performs poorly when the projection data contains significant noise.

Why?

Are we missing something in the design of the FBP or BPF methods?

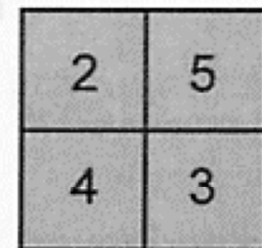
Basic Problem of Image Reconstruction



problem

$$\begin{aligned}A + B &= 7 \\A + C &= 6 \\A + D &= 5 \\B + C &= 9 \\B + D &= 8 \\C + D &= 7\end{aligned}$$

method



solution

FIGURE 13-27. The mathematical problem posed by computed tomographic (CT) reconstruction is to calculate image data (the pixel values—A, B, C, and D) from the projection values (arrows). For the simple image of four pixels shown here, algebra can be used to solve for the pixel values. With the six equations shown, using substitution of equations, the solution can be determined as illustrated. For the larger images of clinical CT, algebraic solutions become unfeasible, and filtered backprojection methods are used.